2017

Genome-Scale CRISPR-Cas9 Knockout Screen Identifies HUWE1 as a Modifier of EGFR Dependence in Non-Small Cell Lung Cancer Cells

Jon DiMaina
Medical University of South Carolina

Genome-scale CRISPR-Cas9 knockout screen identifies HUWE1 as a modifier of EGFR dependence in non-small cell lung cancer cells

by

Jon DiMaina

A thesis submitted to the faculty of the Medical University of South Carolina in partial fulfillment of the requirements for the degree of Masters of Biomedical Sciences in the College of Graduate Studies

Department of Pathology and Laboratory Medicine, 2017

Approved by:

(Chairman, Brad Shulte)

(Victoria Findlay)

(Steve Ethier)

(Bob Gemmill)

(John Wrangle)

(Major Advisor, Hiu Wing Cheung)

Copyright Page

Abstract

Non-small cell lung cancers (NSCLC) with epidermal growth factor receptor (EGFR) gene mutations can exhibit a strong dependence on mutant EGFR signaling for growth and survival. They are also sensitive to EGFR tyrosine kinase inhibitors (TKIs), which provide superior clinical benefits to conventional chemotherapy. However, despite initial response, most patients experience relapse with resistant tumors within a year. This study aims to identify modifiers of dependence on mutant EGFR signaling and the mechanisms by which they do so in order to improve therapeutic strategies and outcomes.

A genome-scale CRISPR-Cas9 genetic knockout screen was conducted to identify genes whose loss-of-function confer EGFR-TKI resistance. A pooled sgRNA library targeted more than 18,000 protein-coding human genes with multiple sgRNAs. The lung cancer cell line HCC827 was used as it is EGFR-mutant and sensitive to EGFR TKIs. Cells were transduced with the sgRNA library and cultured in the presence of erlotinib, an EGFR TKI, or DMSO control for 17 days. sgRNAs that were enriched in erlotinib-treated groups over control groups were identified, indicating genes whose loss-of-function confer TKI resistance. The RNAi gene enrichment ranking (RIGER) algorithm was applied to identify gene hits with enrichment of multiple sgRNAs.

Top-ranked candidates include previously confirmed genes *PTEN*, *NF1*, *NF2*, *TSC1*, and *TSC2;* validating this system as a means to identify modifiers of EGFR dependence in HCC827 cells. A novel candidate gene is the E3 ubiquitin ligase HUWE1. I showed that suppression of HUWE1 by inducible short hairpin RNA (shRNA) in HCC827 cells re-activated AKT and ERK1/2 signaling pathways and increased cell survival in response to EGFR inhibition. These findings were confirmed *in vivo* by implanting mouse xenografts of HCC827 cells with suppressed HUWE1 expression and

monitoring tumor development in response to erlotinib. Tumors with suppressed HUWE1 continued to grow into large tumors whereas control cells had durable tumor regression throughout the treatment period.

We have shown that dependence on EGFR signaling can be decreased in EGFR-mutant lung cancer cells through mechanisms that involve the activation of AKT and ERK1/2 signaling pathways. Future studies involve identifying HUWE1 substrates/interactions that participate in tumor cell response to EGFR inhibitors, revealing a novel mechanism of resistance to EGFR-targeted therapy.

Table of Contents:

Abstract iii

List of Tables vii

List of Figures viii

List of Abbreviations x

Acknowledgements xiii

Background and Introduction 1

Lung Cancer Statistics 1

Lung Cancer Subtypes 1

NSCLC Treatment Strategies 2

Driver Mutations in NSCLC 2

The EGFR Signaling Pathway 3

Mutant EGF-receptors Escape Negative Regulation 5

Molecular Predictors for Response to TKIs 6

Toxicities of EGFR-TKI Therapy 7

Acquired Resistance to EGFR-TKIs 8

PI3K/AKT and ERK1/2 signaling in the regulate cell proliferation and survival 11

BIM induction is critical for EGFR-TKI response 14

The ubiquitin-proteasome system 16

Acquisition versus Selection Model of Acquired Resistance 18

Addressing Resistance in the Clinic 20

Identification of modifiers of EGFR signaling dependence 23

Preliminary Data 24

Research Plan 27

Rationale for the study of HUWE1 27

Hypothesis 29

Specific Aim #1 29

Experimental Design 30

Results 37

Discussion and Alternative Approaches 51

Specific Aim #2 54

Experimental Design 54

Results 57

Discussion and Alternative Approaches 63

Future Experiments 65

Significance of Study 69

References 70

List of Tables:

Table 1: shRNA targeting sequences for HUWE1 knockdown 31

Table 2: qPCR primers 35

List of Figures:

Figure 1: The EGFR signaling pathway 4

Figure 2: Mutations in the kinase domain of EGFR 6

Figure 3: Chemical structure of first generation EGFR-TKIs 7

Figure 4: Molecular pathways involved in EGFR-TKI resistance 11

Figure 5. Interactions within the BCL2 family 15

Figure 6. The ubiquitin cascade and chain formation 18

Figure 7: “Acquisition” versus “selection” model of resistance 19

Figure 8: Chemical structure of osimertinib 21

Figure 9: sgHUWE1 is enriched in cells positively selected for by erlotinib 26

Figure 10: shRNA targeting HUWE1 suppresses protein and mRNA expression 37

Figure 11: Suppression of HUWE1 decreases sensitivity to erlotinib 38

Figure 12: Suppression of HUWE1 attenuates apoptosis 39

Figure 13: Suppression of HUWE1 does not affect cell cycle 41

Figure 14: Suppression of HUWE1 reactivates AKT and ERK1/2 43

Figure 15: Inhibition of PI3K or MEK suppress HUWE1 loss-induced resistance 45

Figure 16: Suppression of HUWE1 increases SHOC2 and c-MYC and decreases BIM levels 47

Figure 17: Gene set enrichment analysis plot 49

Figure 18: Heat map of genes differentially expressed by HUWE1 suppression 50

Figure 19: Timeline of xenograft experiment 57

Figure 20: Suppression of HUWE1 increases tumor volume and weight in vivo 59

Figure 21: Suppression of HUWE1 reactivates AKT and ERK1/2 in vivo 61

Figure 22: Suppression of HUWE1 increases tumor proliferation and survival in vivo 63

List of Abbreviations

AE—adverse events

Akt—v-akt murine thymoma viral oncogene homolog

ATP—adenosine tri-phosphate

BIM—BCL2 interacting mediator of cell death

BRAF—v-Raf murine sarcoma viral oncogene homolog B

CAMPK-- calcium/calmodulin-dependent protein kinase

CRISPR—clustered regularly interspaced palindromic repeats

DAG—diacylglycerol

DMSO—dimethyl sulfoxide

Dox—doxycycline

EGF—epidermal growth factor

EGFR—epidermal growth factor receptor

ERBB3—Erb-B2 receptor tyrosine kinase 3

ERK—Extracellular signal regulated kinase

FACS—fluorescence-activated cell sorting

Grb2—growth factor receptor-bound protein 2

GSEA—Gene set enrichment analysis

HER2—human epidermal growth factor receptor 2

HGF—hepatocyte growth factor

HSP90—heat shock protein-90

IGF1—insulin-like growth factor 1

MAPK—mitogen-activated protein kinase

MEK—mitogen-activated protein kinase

MOI—multiplicity of infection

mRNA—messenger RNA

mTOR--mechanistic target of rapamycin

NF-κB—nuclear factor kappa-light-chain-enhancer of activated B cells

NMD—nonsense mediated decay

NSCLC—non-small cell lung cancer

ORF—open reading frame

ORR—overall response rate

PCR—polymerase chain reaction

PI3K--phosphoinositide-3-kinase

PI3KCA—Phosphatidylinositol-4,5-Bisphosphate 3-Kinase Catalytic Subunit Alpha

PIP3--phosphatidylinositol-3,4,5-trisphosphate

PFS—progression-free survival

PKC—protein kinase C

PLCγ--phospholipase C gamma

PTB—phosphotyrosine binding

PTEN—phosphatase and tensine homolog

Raf—Raf murine viral oncogene homolog

Ras--Ras viral oncogene homolog

RECIST—Response Evaluation Criteria in Solid Tumors

RTK—receptor tyrosine kinase

SCLC—small-cell lung cancer

sgRNA—single-guide RNA

SH2—Src homology 2

SOS—son of sevenless homolog

STAT-- signal transducer and activator of transcription

TGFα—transforming growth factor alpha

TKI—tyrosine kinase inhibitor

WHO—World Health Organization

Acknowledgements

I would like to thank the lab of Dr. Hiu Wing Cheung for providing the preliminary data, resources, and training to make this thesis possible. I would also like to thank the other members of my committee, Dr. Bob Gemmill and Dr. Steven Ethier; I am very fortunate to have such a high level of expertise involved in my project. Dr. John Wrangle, for taking time out of your busy schedule to offer your perspective as a clinician. I have been fascinated by our discussions and I have no doubt they will continue to inspire me well into the future.

I would also like to especially thank Dr. Victoria Findlay. You were my first contact at MUSC and the reason I applied. You took a chance on me and made this experience possible. You have offered your support as a mentor and as a friend. I am most certain that I would not be in this position without you.

I would also like to thank the Department of Pathology and Laboratory Medicine and the Medical University of South Carolina for providing a learning and training environment surrounded by so many talented individuals.

Funded by: Department Start-up Fund (H.W.C)

Introduction and Background

Lung cancer statistics

Lung cancer is the leading cause of cancer-related deaths in both men and women in the United States, accounting for 27% of cancer deaths in 2016 and an estimated 220,000 new cases [1]. The leading risk factor for lung cancer is cigarette smoking , accounting for 82% of lung cancer deaths in the United States [2]

The overall 5-year survival rate is 17.4% and for those with stage IV disease at diagnosis, this rate drops to a dismal less than 2%. Unfortunately, most patients are diagnosed with advanced-stage disease [3]. Unlike other cancer types, which have seen a combined 5-year relative survival rate increase of 20%, lung cancer survival rates have seen only marginal increases over the past four decades, as the 5-year survival rate was 12% in 1977 [1]. The advent of low-dose helical computed tomography, however, has resulted in earlier detection and may help to raise survival rates and reduce lung cancer mortality [4].

Lung cancer subtypes

Lung cancers can be derived from neural crest cells, which develop into small-cell lung cancer (SCLC), or epithelial cells, which develop into non-small cell lung cancers. NSCLC can be further divided into adenocarcinoma, squamous cell carcinomas, large cell carcinomas, and sarcomatoid carcinomas. Approximately 80% of lung cancers are NSCLC and approximately 60% of NSCLC are adenocarcinomas [1]. The various lung cancer subtypes have resulted in a diversity of treatment strategies due to their intrinsically different sensitivities to distinct agents.

NSCLC treatment strategies

Treatment decisions for NSCLC patients are based on histomorphological, immunohistochemical, and molecular characterizations. Until recent advances in TKI therapy, the standard first-line treatment for non-resectable NSCLC has been cisplatin-based chemotherapy regimens. However, standard chemotherapy regimens provide only modest clinical benefit with significant toxicities [5, 6].

Driver mutations in NSCLC

Emerging treatment strategies for molecular subsets of NSCLC are based on specific driver mutations. Tumor formation often involves the acquisition of multiple mutations that activate growth-enhancing genes (oncogenes) or inactivate growth-inhibitory genes (tumor suppressor genes). Epigenetic (non-mutational) abnormalities affecting oncogenes and tumor suppressor genes can also contribute to tumorigenesis [7].

Despite harboring a complex set of genetic lesions contributing to tumor formation, cancers may rely on single-mutant oncogenes for survival, a concept known as "oncogene addiction" [8]. Identification of mutant oncogenes that tumors rely on for growth and survival has therapeutic relevance as their dependence on mutant oncogenes can be exploited with targeted agents. Perhaps the best case of clinical evidence of oncogene addiction is the targeting of the *Bcr-Abl* oncogene in chronic myeloid leukemia with the small-molecule inhibitor imatinib, which in one study induced a complete hematologic response in 95% of patients in whom previous interferon therapy had failed [9].

The most frequent driver mutations found in NSCLC affect K-Ras and EGFR, occurring in a mutually exclusive manner [10]. Oncogenic EGFR driver mutations are most frequently found in the NSCLC adenocarcinoma histology (95%) with incidence rates ranging from ~15% in Caucasians to ~50% in East Asians [11].

The EGFR signaling pathway

The EGFR family of tyrosine kinases consists of four members: EGFR (HER1/ErbB1), HER2 (ErbB2), HER3 (ErbB3), and HER4 (ErbB4). The EGFR signaling pathway (Figure 1) regulates physiological processes involved in cell proliferation, apoptosis, motility and neovascularization and its dysregulation has been associated with tumorigenesis [12].

Ligands of the EGF-receptor include EGF, TNFα, and amphiregulin, which bind specifically to EGFR. Betacellulin, heparin-binding growth factor, and epiregulin bind to both EGFR and ErbB4. Neuroregulins bind specifically to ErbB3 and ErbB4. ErbB2 has no direct ligand but heterodimerizes with all other family members upon ligand binding [13, 14].

Upon ligand binding to the EGF-receptor, homo- or hetero-dimers are formed, leading to subsequent receptor activation of the intracellular kinase domain. Tyrosine residues are phosphorylated within the cytoplasmic tail and serve as docking sites for proteins containing Src homology 2 (SH2) and phosphotyrosine binding (PTB) domains, resulting in the activation of intracellular signaling pathways [15, 16]. ErbB hetero-dimerization allows for signal amplification and diversification but ErbB2 is the preferred heterodimer partner for all other ErbB receptors [17]. In addition, ErbB3 has an impaired

kinase domain, thus despite ligand binding, ErbB3 only functions when in complex with another ErbB family member [18].

The signaling pathways initiated by activated EGFR include the Ras/Raf/MEK pathway through either Grb2 or Shc adaptor proteins and PI3K/AKT by recruiting the p85 regulatory subunit [19]. EGFR signaling can also induce signal transducer and activator of transcription (STAT) factors [20].

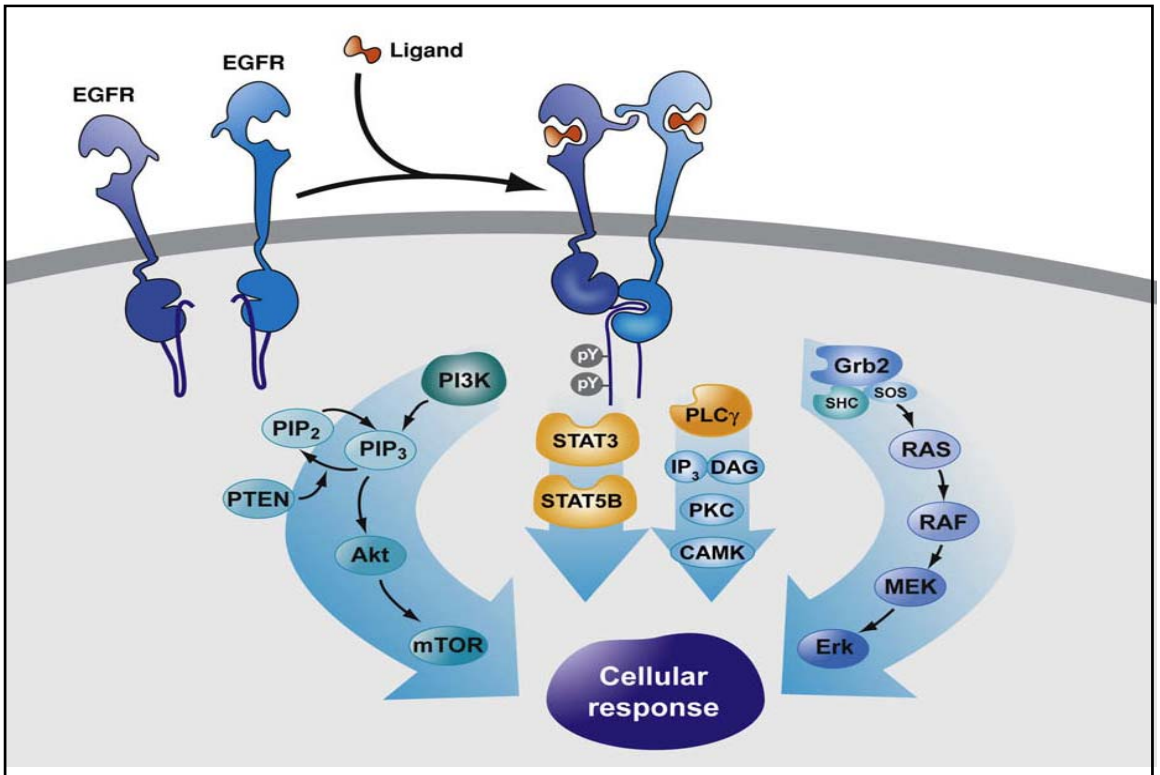

Figure 1. The EGFR signaling pathway. In the absence of ligand, the receptor exists in monomeric form with the carboxyl-terminal tail of the receptor, auto-inhibiting the kinase domain. Ligand binding promotes dimer formation, resulting in a conformational change which allows for intracellular trans-phosphorylation of tyrosine residues that serve as docking sites for signaling adapters, intracellular enzymes, or transcription factors. As such, activated EGFR is involved in a myriad of signaling pathways involved in cell proliferation, survival, and migration. Figure adapted from "Oncogenic mutant forms of EGFR: Lessons in signal transduction and targets for cancer therapy" by G. Pines, W. Kostler, and Y. Yarden, 2010, FEBS Lett, 2010. 584(12): p. 2699-706. Copyright 2015 Federation of European Biochemical Societies. Adapted with permission [21].

Mutant EGF-receptors escape negative regulation

The most common mutations seen in EGFR-mutant NSCLC are an in-frame deletion in exon 19 (44%), which encodes the phosphate-binding loop, and a CTG to CGG point mutation in exon 21, which encodes the activation loop, resulting in the substitution of leucine by arginine at codon 858 (42%). Other oncogenic mutations include a point mutation in exon 18, mainly G719X (X indicates A, C, S, or D), which occurs at a frequency of approximately 4%; insertion mutations in exon 20, which encodes the α-C helix (4%); and additional point mutations in exon 21 other than L858R occur at a frequency of approximately 3% [21] (Figure 2). All of these mutations are believed to destabilize the inactive conformation, leading to increased basal kinase activity despite lack of ligand binding [22]. In addition, kinase-mutated EGF-receptors retain their ability to respond to growth factor ligands including EGF and TGFα, further augmenting signaling activity [23].

Exon 19 of EGFR encodes amino acids 729-761 and most exon 19 deletions occur between amino acids 746-753. These deletions occur in the ß3 strand adjacent to the C-helix, and it has been proposed that the shortening of this strand favors the active conformation [24]. The L858R substitution locks the receptor in a constitutively active state due to the much larger charged side chain of arginine, which cannot be accommodated in the inactive state but is readily accommodated in the active conformation. While much less common, G719X is believed to destabilize the inactive conformation in a similar fashion to induce constitutive signaling [25].

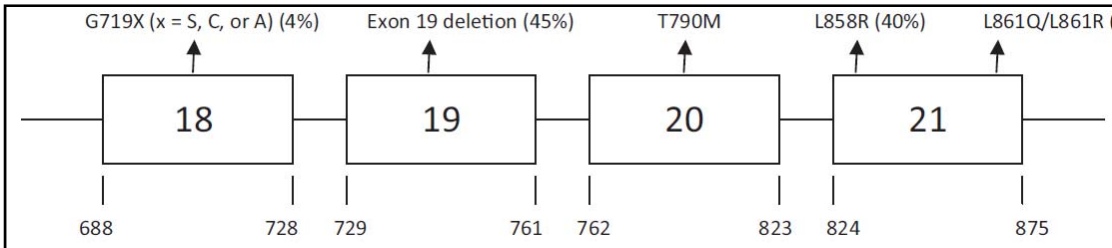

Figure 2. Mutations in the kinase domain (exons 18-21) of EGFR and their associated frequencies of occurrence. With the exception of T790M, these mutations are associated with sensitivity to EGFR-TKIs. T790M is associated with resistance to EGFR-TKIs. Figure adapted from "Tyrosine kinase inhibitors for epidermal growth factor receptor gene mutation–positive non-small cell lung cancers: an update for recent advances in therapeutics" by C. Chung, 2016, J Oncol Pharm Pract, 22(3): p. 461-76. Copyright 2016, SAGE Publications. Adapted with permission [26].

Molecular predictors for response to TKIs

Interestingly, the somatic mutations in the kinase domain of EGFR driving tumorigenesis have a clinical correlation with sensitivity and responsiveness to EGFR-TKIs. EGFR-mutants are 10- to 100-fold more sensitive to EGFR-TKIs versus their wild-type counterpart [27-29]. An exception to this correlation is the exon 20 insertion mutation, which has been shown to be resistant to EGFR-TKI therapy [30].

First generation EGFR-TKIs, such as erlotinib and gefitinib, are effective reversible inhibitors of mutant EGFR, particularly those harboring EGFR exon 19 deletions ($EGFR^{del19}$) or the EGFR exon 21 L858R mutation ($EGFR^{L858R}$). They are currently used as first-line therapies for the treatment of advanced EGFR-mutant NSCLC [31-34]. Erlotinib and gefitinib are quinazoline derivatives (Figure 3) that work as a reversible competitive inhibitor of adenosine tri-phosphate (ATP) for the ATP-binding pocket of the intracellular tyrosine kinase domain of the EGF-receptor.

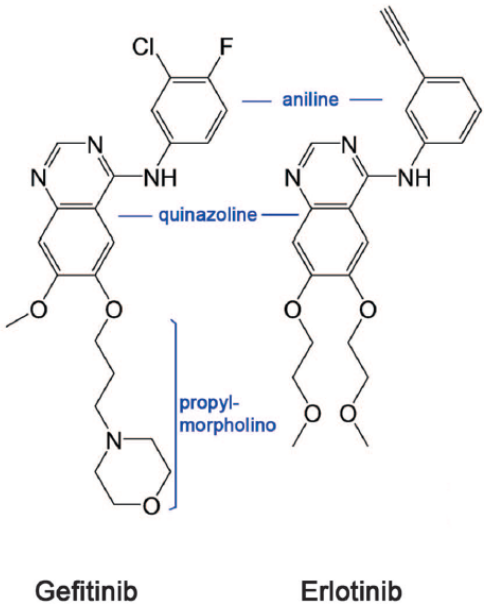

Figure 3. Chemical structure of first generation EGFR-TKIs gefitinib (left) and erlotinib (right). Figure adapted from "The T790M mutation in EGFR kinase causes drug resistance by increasing the affinity for ATP" by Yun et al., 2008, Proc Natl Acad Sci U S A, 105(6): p. 2070-5. Copyright 2008 National Academy of Sciences [35].

Patients harboring EGFR-mutant NSCLC when given EGFR-TKIs as a first-line therapy have experienced objective response rates of approximately 70% and a median progression-free survival (PFS) of 9-12 months, a significant improvement over chemotherapy in unselected NSCLC patients [36-38]. Multiple phase III trials have demonstrated EGFR-TKI therapy superior to chemotherapy alone in terms of response and PFS [31-33, 39, 40]. Additionally, durable responses have been achieved when EGFR-TKI therapy has been given in second or third-line settings as well [41-43].

Toxicities of EGFR-TKI therapy

Toxicities of EGFR-TKI therapy are often less severe than those associated with traditional cytotoxic chemotherapy, but adverse events (AE) have occurred. EGFR-TKI-

associated rash, or follicular acneiform eruption, is the most common clinical AE (63%) and typically manifests on the face, shoulders, and back but tends to improve over time despite with continued EGFR-TKI therapy [44]. The second most common AE associated with EGFR-TKI therapy is diarrhea, which is thought to result from excess chloride secretion and is reported in 40 to 60% of patients. However, diarrhea rarely results in disruption of treatment [45].

Acquired resistance to EGFR TKIs

Despite initial response to EGFR-TKI therapy, most patients develop disease progression after 9-14 months of treatment. Clinical criteria for diagnosis of acquired resistance have been proposed by Jackman et al., to include:

1) Previous treatment with a single-agent EGFR-TKI to assess its therapeutic contribution to tumor response alone;

2) A tumor that harbors an EGFR mutation that induces EGFR-TKI sensitivity (exon 19 deletion, L858R, G719X, L861Q) OR objective clinical benefit from EGFR-TKI treatment defined as partial or complete response (Response Evaluation Criteria in Solid Tumors [RECIST] or World Health Organization [WHO] Handbook for Reporting Results of Cancer Treatment) or stable disease of greater than six months (RECIST or WHO) after EGFR-TKI initiation;

3) Disease progression (RECIST or WHO) while on continuous treatment of EGFR-TKI within 30 days prior; and

4) No intervening systemic therapy between EGFR-TKI cessation and initiation of new therapy [46].

Granted, some lung cancer patients who invariably develop acquired resistance to EGFR-TKI therapy do so through pharmacological mechanisms. However, the scope of my study is focused on biological resistance mechanisms, those that reflect the evolution of cancer cells in the presence of the drug. Biological resistance mechanisms to EGFR-TKIs in EGFR-mutant NSCLC typically occur in four ways: 1) genetic alterations in the EGF-receptor render the drug ineffective at continued inhibition of EGFR signaling, 2) bypass signaling renders inhibition of EGFR alone insufficient to preserve tumor control, 3) modulation of downstream effectors of EGFR signaling that influence proliferation and apoptosis, and 4) phenotypic changes such as conversion to SCLC or epithelial-to-mesenchymal transition (Figure 4).

The most clinically relevant mechanism of resistance to first generation EGFR-TKIs is a secondary mutation in the EGFR kinase domain (T790M), which is found in 50-65% of patients at the time of progression [47, 48]. The primary mechanisms by which T790M confers resistance to first-generation EGFR-TKIs such as gefitinib or erlotinib is increasing the binding affinity of ATP to the binding pocket, thereby reducing the potency of the ATP-competitive inhibitor [35]. Early work suggested steric hindrance by the bulky methionine substitution may contribute to T790M resistance [48, 49]. However, efficacy of structurally similar irreversible inhibitors suggests that reduced binding affinity is the primary contributor to resistance conferred by T790M [35].

It is also common for EGFR-mutant NSCLC to develop acquired resistance to TKI therapy by activating bypass signaling pathways that render inhibition of EGFR alone insufficient to control tumor growth. The first described such mechanism was the amplification of MET, a proto-oncogene encoding a receptor tyrosine kinase (RTK) that binds to hepatocyte growth factor (HGF). In this resistance mechanism, EGFR inhibition

is bypassed through amplified MET-mediated ERBB3 signaling [50]. High-level expression of HGF can induce a similar effect, but other growth factors such as EGF, TGFα, and insulin-like growth factor 1 (IGF1) were shown not to promote EGFR-TKI resistance [51]. Overexpression of CRKL, a signal transduction adaptor protein, has been reported to decrease sensitivity to EGFR-TKIs [52]. Increased FAS expression induces NF-κB signaling and has been observed in an acquired resistance cell line model [53]. Other bypass signaling tracks identified in patients with EGFR-TKI resistant tumors harboring drug–sensitive EGFR mutations include PIK3CA mutation, BRAF mutation, and HER2 amplification [47, 54-56].

Induction of pro-apoptotic BCL2 interacting mediator of cell death (BIM) is essential for EGFR-TKI induced apoptosis [57], and pre-treatment BIM levels have been associated with responsiveness to EGFR-TKI [58]. However, germline BIM deletion polymorphisms in two independent cohorts of NSCLC patients failed to correlate objective response rates, progression-free survival, or overall survival between patients with or without a BIM deletion polymorphism [59].

Epithelial to mesenchymal transition (EMT) is a phenomenon in which epithelial cells gain mesenchymal characteristics such as loss of the cell-junction protein E-cadherin and acquisition of vimentin expression and is associated with increased migratory potential [60]. Clinical evidence has shown phenotypic changes consistent with EMT at the time of EGFR-TKI resistance without any other identified mechanism of resistance [54, 61]. However, the frequency of occurrence in the patient population requires additional investigation due to the small size of re-biopsy series available for analysis. Transformation to small cell lung cancer (SCLC) from adenocarcinomas has also been observed in clinical specimens [54] at an estimated frequency of 3-10% [47].

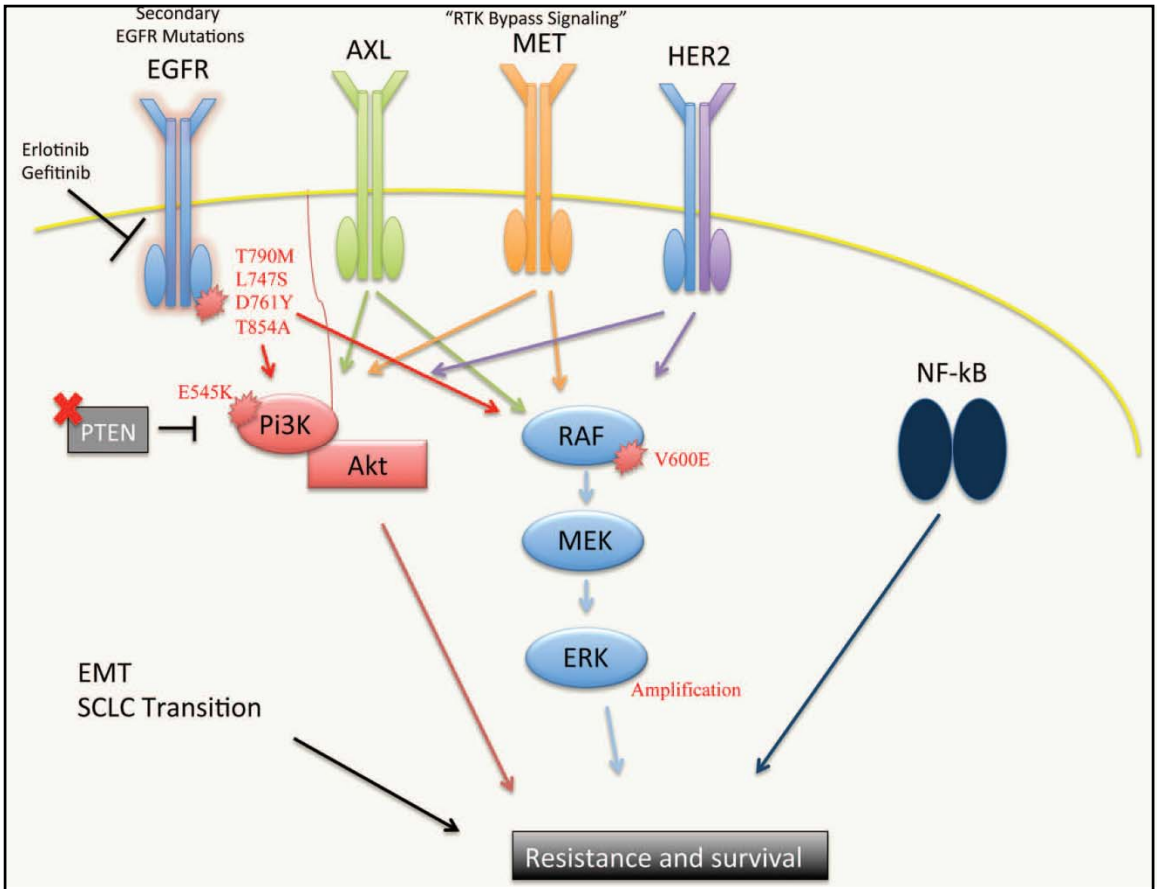

Figure 4. Molecular pathways involved in EGFR-TKI resistance. Secondary mutations in the EGFR kinase domain diminish the ability of first generation EGFR-TKIs to inhibit mutant EGFR signaling. Up-regulation or activation of other RTKs such as AXL, MET, or HER2 can activate downstream effector pathways common to EGFR despite its continued inhibition. RTK independent activation of downstream effector pathways can also occur by PTEN loss, activating PI3K and BRAF mutations. Epithelial-mesenchymal transition (EMT) as well as a small-cell phenotype transition also has been associated with EGFR-TKI resistance. Adapted from "Mechanisms of resistance to EGFR targeted therapies" by G. Hrustanovic, B. Lee, and T. Bivona, 2013, Cancer Biol Ther, 14(4): p. 304-14. Copyright © 2013 Taylor & Francis. Adapted with permission [62].

PI3K/AKT and ERK1/2 signaling regulate cell proliferation and survival

As stated earlier, the signaling pathways initiated by activated EGFR include RAS/RAF/MEK/ERK1/2 and PI3K/AKT. Reactivation of these pathways by bypass

signaling through alternative receptor tyrosine kinases (RTK) or modulation of downstream effectors can provide a mechanism for tumor cells to promote cell survival despite continued EGFR inhibition.

Reactivation of PI3K/AKT signaling by a RTK that bypasses EGFR can occur when the receptor is phosphorylated, providing a docking site for p85, a regulatory subunit of PI3K. The catalytic subunit, p110, is recruited to the complex and the now active PI3K converts phosphatidylinositol (4,5)-phosphate [PI(4,5)P2] into phosphatidylinositol (3,4,5)-phosphate [PI(3,4,5)P3] [63]. This conversion allows for the recruitment of AKT which is then phosphorylated at residues T308 by PDK1, and S473 by mTORC2 (also termed PDK2), initiating the mediation of downstream substrates that regulate cell cycle progression and survival [64].

Reactivation of PI3K/AKT signaling can also occur by modulation of phosphatases that negatively regulate PI3K/AKT activity. In multiple cancer types, it is common to see mutations that result in the loss-of-function of phosphatase and tensin homologue deleted on chromosome 10 (PTEN), or SH2-containing phosphatases 1 and 2 (SHIP1 and SHIP2) [65, 66]. The function of these phosphatases is to convert [PI(3,4,5)P3] back to [PI(4,5)P2], to terminate signaling [67]. Mutations have also been reported in the catalytic subunit of PI3K that result in the constitutive activation of the enzyme [68].

AKT signaling can promote cell survival and proliferation by multiple mechanisms [69] including:

1) Phosphorylation and inhibition of forkhead family transcription factors (FOXO). FOXOs promote growth inhibition and apoptosis by inducing the

expression of pro-apoptotic members of the BCL2 family and cyclin-dependent kinase inhibitors;

2) Activation of NF-κB and CREB transcription factors, inducing the expression of pro-survival genes;
3) Directly phosphorylating and inactivating the pro-apoptotic BCL2 family protein, BAD;
4) Activation of mTOR, a central regulator of cell metabolism, survival and proliferation; and,
5) Maintaining mitochondrial integrity by activating hexokinase.

In a similar fashion to AKT signaling, phosphorylation of RTKs provide docking sites for adapter proteins that initiate the RAS/RAF/ERK signal transduction pathway. The adapter protein growth factor receptor-bound protein 2 (GRB2) recruits the nucleotide exchange factor, son of sevenless (SOS), which in turn activates the GTPase RAS. Activated RAS interacts with RAF, which phosphorylates MEK1 and MEK2, which in turn activate ERK1 and ERK2 [70]. However, RAF activation is complex and involves multiple GTPases, kinases, and phosphatases.

The onset and duration of ERK signaling is regulated, in part, by phosphatases. For example, protein phosphatase 2A (PP2A) can regulate the RAF/MEK/ERK pathways in a positive manner by dephosphorylating negative regulatory sites of RAF, or in a negative manner by dephosphorylating ERK-dependent sites of RAF [70].

Scaffolding proteins, such as SHOC2—which facilitates the association of the RAS/RAF complex [71], can also have a critical role in modulating ERK signaling. It has been recently suggested that regulation of SHOC2 is mediated through ubiquitination by the E3 ubiquitin ligase HUWE1 [72].

RAS/RAF/MEK/ERK signal transduction ultimately leads to modulation of transcription factors that regulate cell cycle progression and apoptosis. Cyclins, cyclin-dependent kinases, cyclin-dependent kinase inhibitors, cytokines and growth factors, BCL2-family proteins, and caspases can all be influenced by ERK-activated transcription factors. ERK can directly phosphorylate and activate c-JUN [73], Ets-like protein [74], and c-MYC [75]. Phosphorylation of RSK, a downstream kinase of ERK, activates the transcription factor, CREB [76]. The transcription factor, NF-κB, can be induced by ERK-mediated activation of IKK. IKK phosphorylates Inhibitor of NF-κB proteins leading to their subsequent degradation which allows NF-κB to translocate to the nucleus for gene transcription [77].

BIM induction is critical for EGFR-TKI response

BIM (also known as BCL2L11) belongs to a subgroup of BCL2-family proteins that contain a BH3 domain and can trigger apoptosis when overexpressed [78]. Mitochondrial outer membrane permeabalization, the hallmark of the intrinsic apoptotic pathway, occurs when the balance of BCL2 family proteins favor the oligermization of the BCL2 family effectors BAX and BAK. Inhibition of BAX and BAK can occur in 3 ways: 1) pro-survival proteins, such as BCL-XL bind to BAX at the outer mitochondrial membrane and translocate it to the cytosol, 2) pro-survival proteins sequester BH3-only proteins to prevent direct activation of BAX and BAK, and 3) pro-survival proteins bind to activated BAX and BAK to prevent their oligermization [79]. A schematic representation of BC2-family protein interactions is shown in Figure 5.

BIM exerts its pro-apoptotic characteristics by either inhibiting pro-survival BH3 members or directly activating BAX or BAK [80]. Ultimately, the balance of the BCL2-family pro-survival and pro-apoptotic proteins determines the cell fate. This dynamic

balance relies heavily upon ubiquitin-mediated proteasome degradation. For example, MCL1, a BCL2 pro-survival protein can rapidly induce apoptosis upon its degradation due to loss of its anti-apoptotic function, and overexpression of MCL1 has been linked to poor prognosis in multiple cancer types [81, 82]. BIM is also subject to proteasome mediate degradation. At the translational level, BIM can be phosphorylated and rapidly degraded by the proteasome. Evidence suggests that ERK1/2-mediated phosphorylation at Ser69 is both necessary and sufficient for proteasome-mediated degradation of BIM [83].

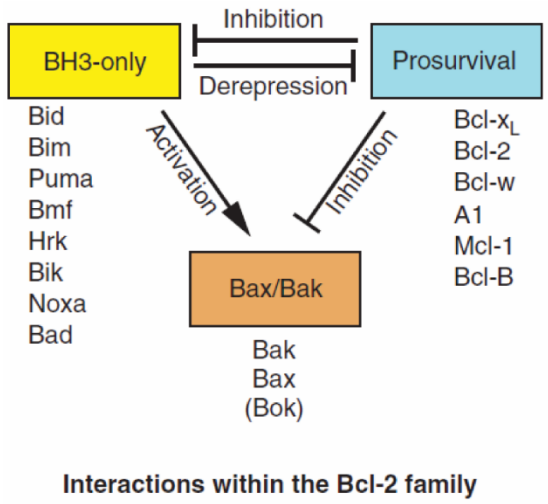

Figure 5. Interactions within the BCL2 family. The BCL2 family of proteins consists of the pro-apoptotic BAX/BAK proteins, pro-apoptotic BH3-only proteins, and pro-survival proteins. The pro-survival proteins inhibit the activity of the pro-apoptotic proteins. BH3-only proteins promote apoptosis by 1) directly activating BAX/BAK or 2) inhibiting the pro-survival proteins. Figure adapted from "Building blocks of the apoptotic pore: how Bax and Bak are activated and oligomerize during apoptosis" by D. Westphal, R. Kluck, and G. Dewson, 2014, Cell Death Differ. Feb; 21(2): 196–205. Copyright © 2013, Nature Publishing Group. Adapted with permission [79].

Three major splice variants exist for BIM protein—short, long, and extra-long (BIM_S, BIM_L, and BIM_{EL}, respectively) with BIM_{EL} being the most predominant in the majority of cell types [78]. Regulation of BIM expression levels can occur at both the transcriptional and translational level. Inhibition of PI3K leads to FoxO3a-dependent transcriptional activation of BIM [84], but comparison of BIM mRNA and BIM proteins

suggests that rapid expression of BIM protein cannot solely be attributed to increases in BIM mRNA following PI3K inhibition [85]. Upon reactivation of AKT, FoxO3a is phosphorylated at Thr32, Ser253 and Ser315, which sequesters FoxO3a to the cytoplasm, preventing its nuclear translocation and subsequent transcription of target genes including BIM [86].

Higher levels of BIM expression are associated with lower risk of mortality and disease progression in EGFR-mutant lung cancer patients [87] and suppression of BIM expression is sufficient to confer in vitro EGFR-TKI resistance [88, 89]. Consistent with these findings, patients with BIM polymorphism deletions (lack pro-apoptotic BH3 domain), which occur in approximately 13% of the East Asian population but are non-existent in African and European populations, have poor clinical outcomes when treated with EGFR-TKI [90].

Thus, reactivation of AKT and ERK1/2, as well as modulation of enzymes that target BCL2-family proteins for proteasome-mediated degradation, may promote EGFR-TKI resistance by providing a mechanism to evade apoptosis via reduced BIM expression.

The ubiquitin-proteasome system

The ubiquitination of proteins can have vast effects on cell physiology and signal transduction, so it stands to reason they are relevant to tumorigenesis and resistance to targeted therapies. Targeting proteins for proteasomal degradation by lysine 48-linked polyubiquitin has been well characterized [91]. Ubiquitylation using other polymerization sites, such as K63, can also have non-degradative function, such as membrane

trafficking, DNA repair and replication, and inflammatory response, through mono-ubiquitination [92] or poly-ubiquitination of non-K48 chains [93].

The ubiquitination machinery consists of three types of enzymes (E1, E2, and E3) that act sequentially to covalently attach ubiquitin onto target substrates via an isopeptide bond. The role of the E1 enzyme is to activate the C-terminal glycine residue of ubiquitin in an ATP-dependent mechanism. Activated ubiquitin is then transferred to a cysteine residue of the E2 enzyme. The E3 enzyme catalyzes the linkage of the ubiquitin to a lysine residue of the substrate protein. Specificity of the target substrate is determined by the E3 enzyme [91].

Classes of E3 ubiquitin ligases are characterized by their conserved structure and the mechanism by which ubiquitin is transferred from the E2 enzyme to the substrate. Really interesting new gene (RING) and Skp1–Cul1–F-box-protein (SCF) families of E3 ubiquitin ligases catalyze the direct transfer of ubiquitin from the E2 to the target substrate. The homology to E6AP C-terminus (HECT) and RING-between-RING (RBR) family of E3 ubiquitin ligases, in contrast, possess intrinsic catalytic activity. In a two-step reaction, the ubiquitin is first transferred to the E3 enzyme, and then directly transferred onto the substrate by the E3 enzyme [94]. A schematic representation of the ubiquitin cascade is shown in Figure 6.

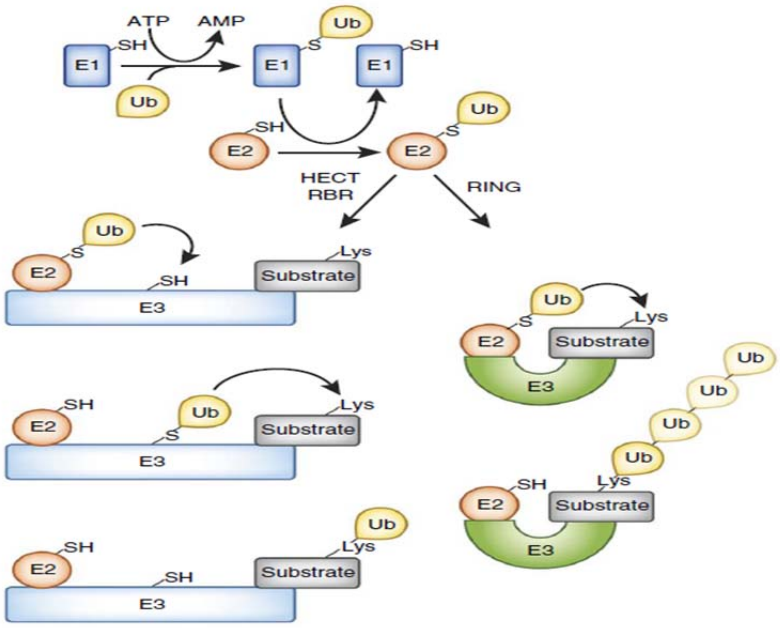

Figure 6. The ubiquitin cascade and chain formation. First, an ATP-dependent reaction results in a thioester bond between the ubiquitin and the active site of the E1 enzyme. Ubiquitin is then transferred to the active site of the E2 enzyme in a transthioesterification reaction. Ring E3 enzymes bind to both the ubiquitin-attached E2 and the substrate and catalyze the attack of the substrate lysine. HECT and RBR E3 enzymes are involved in a two-step reaction involving the formation of a thioester with the E3 enzyme, followed by an attack of the substrate lysine. Figure adapted from "New insights into ubiquitin E3 ligase mechanism" by C. Berndsen and C. Wolberger, 2014, Nat Struct Mol Biol. Apr;21(4):301-7. doi: 10.1038/nsmb.2780.

Acquisition versus selection model of acquired resistance

One could propose two models from which acquired resistance mechanisms develop. The selection model assumes that resistant clones exist prior to treatment that are selected for by EGFR-TKIs. The acquisition model presumes that novel genetic or epigenetic alterations occur during the course of EGFR-TKI treatment. Based on initial reports of pre-progression samples lacking $EGFR^{T790M}$, it was believed that such

alterations were the result of “acquisition” only after exposure to EGFR-TKIs [48, 49]. Another group, however, found that a small fraction of cells were $EGFR^{T790M}$+ within a treatment-naïve tumor and experienced a shorter time to progression, suggesting that while the tumor initially responded to EGFR-TKI therapy, the eventual disease progression was due to the selection of the $EGFR^{T790M}$ clones present within the tumor. There has been much debate over whether the “acquisition” or “selection” models of acquired resistance to EGFR-TKI therapy (Figure 7) is the likely cause of eventual disease progression [95].

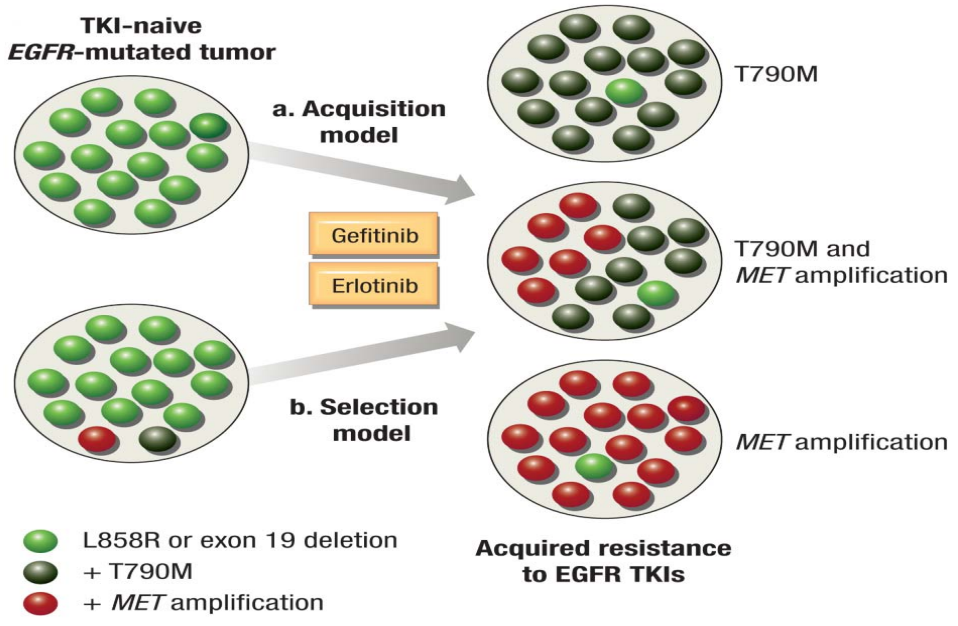

Figure 7. **“Acquisition” versus “selection” model.** T790M and MET amplification mechanisms of acquired resistance after EGFR-TKI treatment in TKI-naïve EGFR-mutant NSCLC. Figure adapted from “Acquired resistance to epidermal growth factor receptor tyrosine kinase inhibitors in non-small-cell lung cancers dependent on the epidermal growth factor receptor pathway” by K. Nguyen, S. Kobayashi, and D. Costa, 2009, Clin Lung Cancer, **10**(4): p. 281-9. Copyright © 2009 Elsevier Inc. Adapted with permission [96].

Addressing resistance in the clinic

There are a number of emerging strategies and ongoing clinical studies that aim to overcome EGF-TKI resistance in the clinic. However, currently the only approved therapy is directed at T790M-mediated resistance.

To address the T790M mechanism of acquired resistance, second generation EGFR-TKIs—including afatinib, neratinib, and dacomitinib were developed to irreversibly bind to EGFR and were shown to more effectively inhibit T790M than first generation EGFR-TKIs [97-99]. However, second generation EGFR-TKIs were not received well in the clinic, with response rates below 10% [100, 101]. The likely explanation for such disappointing results is the lowered IC_{50} against the wild-type receptor which resulted in significant toxicities at doses required to effectively inhibit T790M [97, 99, 102].

Recently, third generation EGFR-TKIs have been developed to target $EGFR^{T790M}$, including osimertinib, a mono-anilino-pyrimidine compound (Figure 8), which received FDA approval in November 2015, the only third generation EGFR-TKI to do so to date. This class of inhibitors forms an irreversible covalent bond at Cys797 in the ATP binding site [103] yet largely spares wild-type EGFR, thus decreasing toxicities and allows for doses that fully inhibit T790M [104].

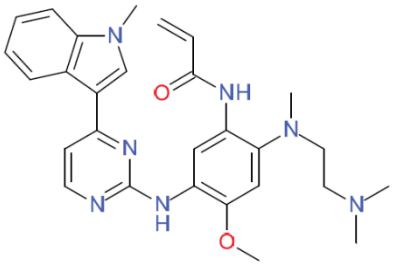

Figure 8. **Chemical structure of osimertinib**. Figure adapted from "AZD9291, an irreversible EGFR TKI, overcomes T790M-mediated resistance to EGFR inhibitors in lung cancer" by D. Cross et al., 2014, Cancer Discov, 4(9): p. 1046-61. ©2014 American Association for Cancer Research. Adapted with permission [104].

Because osimertinib is effective against sensitizing EGFR mutations and is also associated with reduced AE associated with first generation TKIs, it is now being investigated for use in first-line therapy for the treatment of metastatic EGFR-mutant positive NSCLC (AURA phase II expansion cohort, CllinicalTrials.gov, NCT01802632). Two expansion cohorts were given first-line osimertinib monotherapy, and the reported overall response rate (ORR) was 77%. The median progression-free survival was 19.3 months overall, and 3% and 7% of patients developed a ≥3 grade skin rash and ≥3 diarrhea, respectively [105]. A phase II randomized study is ongoing comparing osimertinib with gefitinib and erlotinib as first-line therapies in patients with advance EGFR-mutant NSCLC (FLAURA study, ClinicalTrials.gov, NCT02296125).

Clinical observations have shown that some patients may benefit from retreatment of EGFR-TKI after a period of cessation [106]. This, however, is not a suitable strategy for all patients because a study of patients with acquired EGFR-TKI resistance found that 25% experienced accelerated disease progression immediately following cessation of treatment [107]. A possible explanation is that subclones within

the resistant tumor may remain drug-sensitive but held in a dormant state that rapidly expand upon release of the selective pressure of the EGFR-TKI [108].

Dual inhibition of the extracellular domain of EGFR with monoclonal antibodies and the intracellular domain of EGFR with tyrosine kinase inhibitors have been suggested to provide clinical benefit for resistant tumors mediated by altered drug target mutations such as T790M [109]. Unfortunately, a high incidence of AE may limit its clinical applicability [110].

Heat-shock protein 90 (HSP90) is a molecular chaperone protein that has been shown to play a role in maintaining the active conformation of EGF-receptors and preventing Cbl-mediated ligand-induced receptor down-regulation [111]. Inhibition of HSP90 in combination with EGFR inhibition is being explored as a therapeutic approach for patients with resistant tumors. However, a current phase I/II study was met with significant toxicities and failed to meet its primary endpoint [112].

Anti-angiogenesis agents such as bevacizumab have recently been investigated for clinical efficacy when combined with erlotinib as a first-line therapeutic strategy in EGFR-mutant NSCLC patients. A randomized phase II study found that combining erlotinib plus bevacizumab increased PFS (16.0 months) compared to erlotinib alone (9.7 months). Although there was no significant changes in overall survival, tumor size was significantly reduced in erlotinib plus bevacizumab patients versus erlotinib alone [113]. Additional clinical trials are currently underway to further investigate its use as a first-line regimen (ClinicalTrials.gov, NCT01532089 and NCT01562028).

Targeting immune checkpoints such as PD-1 and PD-L1 has emerged as a promising strategy in lung cancer immunotherapy. Nivolumab, a PD-1-blocking

antibody, has received FDA approval for the treatment of squamous cell lung cancer, but further investigation is needed to determine the efficacy of nivolumab as a monotherapy or in combination with EGFR-TKIs in NSCLC. A phase I trial of nivolumab, a PD-1-blocking antibody found patients that responded obtained durable results [114], but correlating response to EGFR status remains controversial [114, 115]

Despite the success of EGFR TKIs as front-line treatment, acquired resistance is inevitable and remains a significant challenge in the management of patients with EGFR-mutant NSCLC. Therefore, understanding the molecular mechanisms of acquired drug resistance remains a critical step in overcoming drug-resistant tumors in the clinic.

Identification of modifiers of EGFR signaling dependence

Genetic screens using libraries of short hairpin RNA (shRNA) and open reading frames (ORFs) are powerful approaches for identifying novel genes that regulate various phenotypes of cancer cells [116, 117]. Recently, the CRISPR (clustered regularly interspaced short palindromic repeats) and CRISPR-associated endonuclease Cas9 system from *Streptococcus pyogenes* has been harnessed for editing genome or introducing loss-of-function mutations in eukaryotic cells [118, 119]. The Cas9 nuclease can be guided by an engineered single-guide RNA (sgRNA) to cause double-stranded cleavage of a complementary target DNA sequence such as within a coding exon [119]. If the DNA cleavage is repaired by error-prone non-homologous end joining (NHEJ), insertion/deletion (indel) mutations likely occur, resulting in a coding frameshift, generation of premature stop codon, and initiation of nonsense-mediated decay (NMD) of the transcript [119]. Recent studies have successfully utilized Cas9/sgRNA system to

carry out high-throughput genetic knockout screens to identify novel genes that modify dependence on mutant *BRAF* in melanoma cells [120].

Tumor heterogeneity and the complicated mechanisms involved in EGFR-TKI resistance have impeded the development of successful solutions for overcoming this resistance. The use of genetic screens can be used to identify genes that have a critical role in relieving NSCLC cells from EGFR signaling dependence which underlies many resistance mechanisms.

Preliminary Data

Genome-scale CRISPR-Cas9 knockout screen

To identify candidate genes, the Cheung lab applied the RNAi gene enrichment ranking (RIGER) algorithm that used three complementary methods, including: 1) the rank of the top two sgRNAs targeting each gene; 2) the rank of the top two sgRNAs targeting each gene to generate a weighted sum score; and 3) the rank of all sgRNAs targeting each gene using the Kolmogorov-Smirnov (KS) statistics [116]. Among the top 100 highest-ranking candidates nominated by each gene-ranking method, the Cheung lab identified 23 candidate genes that scored in all three analyses.

These 23 highest-ranking candidates included genes previously reported to confer resistance to EGFR-TKIs when expression is suppressed, such as *PTEN*, *NF1*, *NF2*, *TSC1*, *TSC2*, and *MED12* [121-125]. The 23 highest ranking candidates of the sgRNA screen also revealed novel candidates that have not been implicated in EGFR TKI resistance, such as *HUWE1* (Figure 9), BCL2-associated X protein (*BAX*) [126], NF-κB inhibitor zeta (*NFKBIZ*) [53], and c-Src kinase (*CSK*) [127].

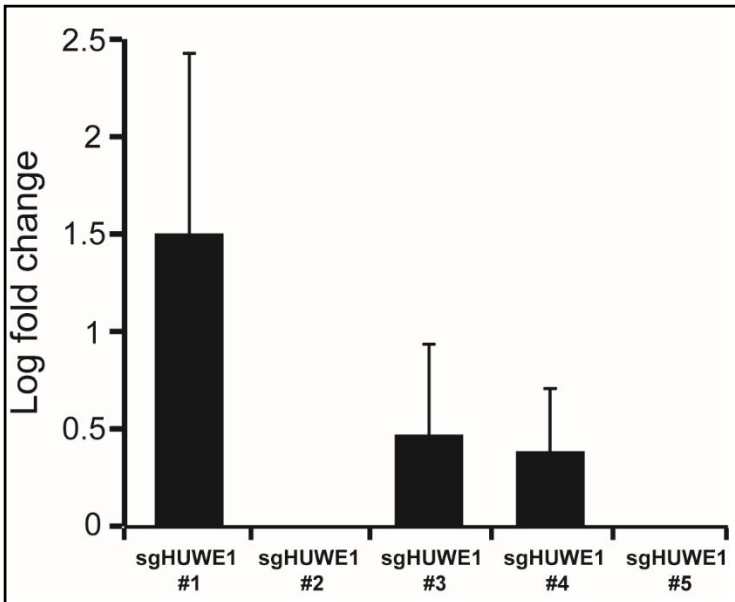

Figure 9. sgHUWE1 is enriched in HCC827 cells positively selected for by erlotinib. Log fold change of 5 sgRNAs targeting different regions of the HUWE1 gene. HCC827 cells were transduced with sgRNA library, treated with erlotinib or DMSO for 17 days and enriched sgRNAs were identified by next-generation sequencing.

Expression profiling of HUWE1-suppressed HCC827 cells

The Cheung lab also performed RNA expression profiling of HUWE1-suppressed HCC827 cells after erlotinib treatment. Doxycycline-inducible shRNA was used for gene suppression and 3 replicates of each treatment group were treated with erlotinib or DMSO control for 24 hours. The treatment groups were as follows: 1) No Dox, No erlotinib; 2) No Dox, Plus erlotinib; 3) Plus Dox, No erlotinib; and 4) Plus Dox, Plus erlotinib. After the treatment period, total cellular RNA was extracted and samples were analyzed on an Illumina HumanHT-12v4.0 bead array at the Hollings Cancer Center Genomics Shared Resource at the Medical University of South Carolina. The

raw data files generated were provided to me for analysis of differential expression between phenotypes.

Research Plan

Rationale for the study of HUWE1

The HECT, UBA, and WWE domain-containing protein 1 (HUWE1), also known as Mule or ARF-BP1, is a HECT (homologous to E6-AP carboxyl terminus)-domain containing ubiquitin E3 ligase. We selected HUWE1 for further study because HUWE1 has been implicated in regulation of cancer cell proliferation and survival but its role in lung cancer response to EGFR-targeted therapy has not been studied.

HUWE1 has been reported to frequently misregulated by overexpression in multiple tumor types including lung cancer (~10%), but was not found to be correlated with overall survival [128]. Mechanistically, HUWE1 has been shown to ubiquitinate and regulate the stability or activity of multiple prominent substrates that are involved in the regulation of apoptosis (such as p53, MCL1), cell proliferation (c-MYC, MIZ1, N-MYC), DNA damage repair (DNA polymerases β and λ), B-cell homeostasis [129, 130], and neural differentiation (N-Myc) [131]. For example, HUWE1 ubiquitinates the anti-apoptotic protein MCL-1 for proteasome-dependent degradation [81]. Suppression of HUWE1 in U2OS osteosarcoma cells stabilizes MCL-1 proteins and protects cells from cisplatin-induced apoptosis [81]. HUWE1 also ubiquitinates MIZ1, a c-MYC binding partner that represses transcription of several cyclin-dependent kinase inhibitors [132]. HUWE1 has been shown to exert growth inhibitory effects on thyroid cancer cells through, in part, regulating p53 stabilization [133]. Inactivation of *Huwe1* in skin of mice

enhances carcinogen- or Ras-induced tumorigenesis due to accumulation of c-MYC/MIZ1 complexes and down-regulation of $p21^{CDKN1A}$ and $p15^{ARF4B}$ [134]. Recently, HUWE1 has been shown to mediate ubiquitination of SHOC2, a scaffold protein that coordinates activation of RAS-RAF1-ERK1/2 signaling cascade [72]. Suppression of HUWE1 in COS-1 fibroblast cells stabilizes SHOC2 proteins and increases RAF1 activity in response to EGF stimulation [72]. HUWE1 also regulates TIAM1 in lung epithelial cells, disassociating cell-cell junctions thereby promoting migration and invasion [135].

With many putative functions, the role of HUWE1 in tumorigenesis is currently still debatable as its determination of cell fate has been described to have both pro- and anti-apoptotic consequences [136]. It remains unexplored whether HUWE1 levels modulate EGFR dependence in EGFR-mutant lung cancer cells. The identification of multiple negative regulators of PI3K-AKT-mTOR signaling pathway in the sgRNA screen suggests that re-activation of this survival pathway allow HCC827 cells to escape from erlotinib-induced growth arrest.

Hypothesis: I hypothesize that suppression of HUWE1 confers EGFR-TKI resistance by reactivating AKT and ERK1/2 signaling pathways to attenuate apoptotic cell death and increase cell proliferation.

Specific Aim #1: **Assess the in vitro effects of suppressing HUWE1 by shRNAs on proliferation and survival in response to EGFR-TKI**. In preliminary data, EGFR-mutant and EGFR-TKI-sensitive cells were enriched with multiple sgRNAs targeting HUWE1 when under positive selection by erlotinib treatment. These results suggest that its loss-of-function may contribute to EGFR-TKI resistance by allowing signaling to continue in the presence of the inhibitor. I will validate the phenotype observed in the sgRNA screen and elucidate underlying mechanisms to better characterize the role of HUWE1 in the modulation of EGFR dependence in EGFR-mutant NSCLC.

Task #1: Establish stable HCC827 cell line expressing inducible shHUWE1 and assess the following:

1. Effects on cell viability in response to erlotinib
2. Effects on apoptosis in response to erlotinib by Annexin V FACS analysis
3. Effects on proliferation in response to erlotinib by BrdU incorporation during DNA synthesis

Task #2: Investigate mechanism of drug resistance by:

1. Examining protein levels downstream of EGFR and of HUWE1 substrates such as phospho-AKT, phosphor-ERK1/2 and MCL1, SHOC2
2. Gene-set enrichment analysis of transcriptional profiling of HUWE1 suppressed HCC827 cells versus control cells in response to erlotinib

Experimental Design

Cell culture: HCC827 cells were cultured in RPMI medium (Corning) supplemented with 10% fetal bovine serum (FBS; Corning) and 1× Penicillin-Streptomycin (Corning). Tetracycline-free FBS (Clontech) was used when tetracycline inducible expression system (TetOn) was applied. 293T packaging cells were cultured in DMEM medium (Corning) supplemented with 10% FBS (Corning).

Chemicals: Erlotinib, BEZ235 and AZD6244 were purchased from Selleck Chemicals. All chemicals were dissolved in DMSO.

Generation of stable cell line expressing TetOn-shHUWE1: The shRNAs were cloned into pLKO-TetOn-shRNA vector [52] (Table 1). Freshly thawed 293T cells were passaged at least three times before viral production and then 1×10^6 were seeded onto 6-cm dishes in 4.5 mL of DMEM + 10% FBS for 24 hours. Opti-MEM (Fisher Scientific) and Mirus TransIT-LT1 transfection reagent (Fisher Scientific) were added to 1 µg of pLKO-TetOn-shHUWE1 or 1 µg pLKO-TetOn-Control, 1 µg of psPAX2 packaging plasmid, and 0.4 µg of VSVG envelop plasmid according to manufacturer's directions. The transfection mixture was incubated at room temperature for 20 minutes before adding drop wise to the 293T cells. The following day, the media was replaced with fresh DMEM + 10% FBS and incubated for an additional 24 hours. Virus was then harvested by passing supernatant through a 0.45 µm filter (VWR).

One day prior to infection, HCC827 cells were seeded in 10-cm dishes to 30-50% confluence at the time of infection. At the time of infection, 1 mL of media was replaced with 1 mL of pLKO-TetOn-HUWE1 or control virus and media was supplemented with 8 µg/mL of polybrene and incubated for 24 hours. An additional non-

infected plate was used as a selection control. Media was then removed and replaced with fresh media supplemented with 2 μg/mL puromycin. Cells were selected for 6 days, changing media + puromycin every three days.

Table 1. shRNA targeting sequences for HUWE1 knockdown	
shRNA	**Target sequence**
shGFP control	5'-ACAACAGCCACAACGTCTATA-3'
HUWE1	5'-CGACGAGAACTAGCACAGAAT-3'

Viability of HCC827 cells expressing shHUWE1 in response to EGFR-TKI: HCC827 cells stably expressing with pLKO-TetOn-control shRNA or pLKO-TetOn-shHUWE1 were cultured, as previously described. Afterwards, 3,000 cells were plated into each well of 96-well plates in the presence or absence of doxycycline (0.5 μg/mL) for 72 hours. Cells were then treated with increasing concentrations of erlotinib (0, 0.001, 0.0033, 0.01, 0.033, 0.1, 0.33, 1, 3.3, and 10 μM) for another 72 hours. The cell viability was determined by using CellTiter-Glo luminescent cell viability assay (Promega) according to manufacturer's instructions. Luminescence (560 nm emission wavelength) was quantified on a SpectraMax M3 microplate reader (Molecular Devices).

Apoptosis in response to EGFR-TKI: HCC827 shHUWE1 cells (2.5×10^5) were seeded into 6-cm culture dishes in the presence or absence of doxycycline (0.5 μg/mL) for 3 days. Erlotinib (1 μM) or an equal volume of DMSO was added and incubated for 24 hours. Cells were then trypsinized and collected together with the cell culture supernatant. After centrifugation at 1500 rpm for 5 min, cell pellets were rinsed with cold 1x PBS. After another centrifugation, cells were resuspended in Annexin binding buffer

and counted. In a volume of 200 µL, 2×10^5 cells were mixed with 10 µL of Annexin V/ AlexaFluor 488 conjugate (Life Technologies) and incubated for 15 minutes at room temperature. After staining, 200 µL of Annexin binding buffer and 4 µL of propidium iodide (100 µg/mL) (Fisher Scientific) were added and incubated for another 20 minutes. Cells were immediately analyzed by flow cytometry on FACSAria IIu (BD Biosciences) and data was analyzed using FACSDiva™ 6 software (BD Biosciences).

Cell Proliferation in response to EGFR-TKI: HCC827 shHUWE1 cells (2.5×10^5) were seeded into 6-cm culture dishes in the presence or absence of doxycycline (0.5 µg/mL) for 3 days. Erlotinib (1 µM) or equal volume of DMSO were added to fresh media and incubated for 24 hours. BrdU (10 µM) was added to the culture medium and cells were incubated for 1 hour at 37°C. Cells were then trypsinized and collected, then centrifuged at 1500 rpm for 5 minutes followed by a wash with 1x PBS and re-centrifugation. Cells were fixed by adding 5 mL of 70% ethanol pre-chilled to -20°C drop-wise to cell pellet while vortexing. Cells were incubated for 20 min at room temperature then stored at 4°C overnight. Cells were then washed in 1x PBS. After centrifugation at 1500 rpm for 5 min, cell pellet was resuspended in 2 mL HCL (2 M) an incubated at room temperature for 20 minutes. After another wash and centrifugation, cell pellet was resuspended in 2 mL of $Na_2B_4O_7$ (0.1M) and incubated for 2 minutes.

Immunoblot protein analysis: To assess protein content of HCC827 cells expressing shHUWE1 in response to EGFR-TKI, an immunoblot analysis was performed. In 6-cm dishes, 2.5×10^5 cells were seeded in the presence or absence of doxycycline (0.5 µg/mL) for 3 days. Erlotinib (0.1, 1, or 10 µM) or DMSO was added to culture media for 6 hours. The media was then aspirated, and cells were rinsed twice with 5 mL ice-cold PBS. Cells were collected in 60 µL RIPA lysis buffer + Halt

phosphatase inhibitors (Pierce using a cell scraper and transferred to a 1.5 mL tube and incubated on ice for 20 minutes. Samples were then centrifuged at 13500 rpm for 20 minutes at 4°C, and supernatant was transferred to a new 1.5 mL tube and gently vortexed. Protein concentrations of samples were assessed using BCA protein assay (Pierce). A volume of 100 µL of BCA protein assay reagent (mixed according to manufacturer's instructions) was added to each well in a 96-well plate. 0, 1, 2, 4, and 6 µL of a 2 mg/mL standard of BSA was used to generate a standard curve. A volume of 2 µL of the samples of unknown concentration was added to each well. The plate was incubated for 30 minutes in the dark at 37°C and then immediately read on a M3 SpectraMax microplate reader (Molecular Devices) at a primary wavelength of 540 nm to determine protein concentrations.

For immunoblot analysis, 25 µg of protein sample was added to a tube containing SDS sample buffer (Life Technologies) plus 10% ß-mercaptoethanol and boiled for 5 minutes. The proteins in the sample were separated using 4-12% NuPage Bis-Tris precast polyacrylamide gels (ThermoScientific) in running buffer containing MOPS SDS running buffer (Life Technologies) and run at 140 volts for 90 minutes. The gels were removed from their cast and transferred to a nitrocellulose membrane using the iBlot dry blotting system (ThermoScientific) according to manufacturer's instructions. For HUWE1 protein analysis, gels were incubated for 10 minutes in a buffer containing NuPage Transfer buffer (Invitrogen) and 0.25% methanol prior to transfer. To reduce non-specific binding, membranes were incubated in 10% milk in PBST for 1 hour. After blocking, membranes were washed 3 times for 5 minutes with PBST and then incubated with primary antibodies and incubated overnight at 4°C with gentle rocking.

Antibodies were diluted in 5% milk as follows: HUWE1 (1:10000, Bethyl); EGFR (1:2000, Cell Signaling); p-ERK1/2 (1:2000, Cell Signaling); total ERK1/2 (1:4000, Cell Signaling); p-AKT 1:20000, Cell Signaling); total AKT (1:4000, Cell Signaling); p-RAF1; total RAF1; SHOC2; c-MYC (1:200, Santa Cruz); MIZ1 (1:200, Santa Cruz); BIM (1:2000, Cell Signaling); and MCL1 (1:1000, Cell Signaling). Membranes were then washed with PBST 3 times for five minutes each. Anti-rabbit and anti-mouse HRP-linked secondary antibodies (Bio-Rad) were diluted in 5% milk (1.5:10000 for all). Blots were incubated in appropriate secondary antibody at room temperature for 1 hour and 30 minutes with gentle rocking. Blots were covered with Enhanced Chemiluminescence Plus blotting substrate (Pierce) for five minutes to activate horseradish peroxidase. Proteins were visualized using CL-Xposure autoradiography film (Pierce) at various time exposures developed on an automatic developer (Kodak). To assess loading control, membranes were stripped by washing membranes in PBST for five minutes followed by distilled water for five minutes and then incubated with 0.2 M NaOH for seven minutes. After washing with distilled water (three times for 5 minutes each) and PBST (once for 5 minutes), blots were incubated with HRP-conjugated ß-actin (Bio-Rad) diluted in 5% milk at 1:2000 for 30 minutes at room temperature with gentle rocking. The blots were then washed and developed as previously described.

Real-time quantitative Reverse-Transcription PCR: HCC827 cells stably expressing with pLKO-TetOn-control shRNA or pLKO-TetOn-shHUWE1 were cultured, as previously described, in 6-cm dishes. After aspirating off media, total RNA was extracted with 1 mL TRIzol reagent (Life Technologies). After incubating for 5 minutes at room temperature, 0.2 mL of chloroform (Sigma) was added followed by 15 seconds of vigorous shaking. Tubes were incubated for additional 3 minutes at room

temperature followed by centrifugation at 12000xg for 10 minutes at 4°C. The colorless layer was then transferred to a new 1.5 mL tube and 0.5 mL of isopropanol (Sigma) was added and incubated for 10 minutes followed by centrifugation at 12000xg for 10 minutes at 4°C. Supernatent was removed, 1 mL of 75% ethanol was added, and the tube was inverted 5 times before centrifugation at 7500xg for 5 minutes at 4°C. Ethanol was then removed and pellet was dissolved in 50 µL of ultra-pure water (Gibco). First-strand cDNA was synthesized from 2 µg total RNA using Maxima First Strand cDNA Synthesis Kit (ThermoScientific) according to manufacturer's instructions. For quantitative PCR, each primer set (Table 2) was plated in triplicate in a 96-well plate with the use of Maxima SYBR Green qPCR Master Kit (ThermoScientific) according to manufacturer's instructions.

Table 2. Primer sequences for qPCR analysis

GENE	Forward	Reverse	T_p (± 2-5°C)
GAPDH	5'-CCTGTTCGACAGTCAGCCG-3'	5'-CGACCAAATCCGTTGACTCC-3'	67.26°C
HUWE1	5'-ACAGGCCATGCAGAGCTTTAA-3'	5'- CTGGCTAGACTCCGACG-3'	67.26°C

Plates were read on a Roche LightCycler480 with the following conditions: 1) after pre-incubation to 95°C, amplification occurred in a series of 45 cycles of 15 seconds at 95°C then 60 seconds at 60°C, 2) melt-curve analysis was performed immediately following amplification by denaturing at 95°C for 5 seconds, annealing at 65°C for 1 minute, then ramping temperature to 97°C at a rate of 0.11°C/s with 5 acquisitions per °C, and 3) cooling of plate to 40°C. The mean cycle threshold was used for comparative cycle threshold analysis (ABI User Bulletin #2). All mRNA levels were normalized to GAPDH.

TKI drug combination to reverse shHUWE1-mediated resistance: HCC827 cells stably expressing with pLKO-TetOn-control shRNA or pLKO-TetOn-shHUWE1 were cultured as previously described before 3,000 cells were plated into each well of 96-well plates in the presence or absence of doxycycline (0.5 μg/mL) for 72 hours. Cells were then treated with increasing concentrations of erlotinib (0, 0.001, 0.0033, 0.01, 0.033, 0.1, 0.33, 1, 3.3, and 10 μM) alone, erlotinib + 0.5 μM BEZ235, erlotinib + 0.5 μM AZD6244, or erlotinib + 0.5 μM BEZ235 + 0.5 μM AZD6244 for another 72 hours. The cell viability was determined by using CellTiter-Glo luminescent cell viability assay (Promega) as described previously.

Gene set enrichment analysis: Raw data files of array values were obtained from the lab of Dr. Cheung for gene set enrichment analysis. The data set contained reads from three replicate experiments of 4 treatment groups: 1) No Dox, No erlotinib; 2) No Dox, Plus erlotinib; 3) Plus Dox, No erlotinib; and 4) Plus Dox, Plus erlotinib. The raw data file was processed for GSEA analysis using the Gene Pattern (Broad Institute) "PreprocessDataset" module with default values. The processed data was loaded into the GSEA software v2.2.0 (Broad Institute) along with the gene set "c2all.v5.0". The phenotypes "Plus Dox, Plus erlotinib" versus "No Dox, Plus erlotinib" were analyzed using default settings with the exception of "Collapse dataset to gene symbols" was set to "false".

Statistical Analysis: Western blotting was analyzed by densitometry using ImageJ software. Significance of changes in cell viability, apoptotic cell populations, and cell-cycle populations will be determined by two tailed, unpaired student's *t*-test. $P < 0.05$ will be considered statistically significant.

Results

Inducible shRNA targeting HUWE1 suppresses protein and mRNA levels in HCC827 cells

To suppress HUWE1 expression in HCC827 cells, we cloned a shRNA targeting the coding sequence of HUWE1 mRNA into a doxycycline-inducible pLKO lentiviral vector. After treating cells with doxycycline for 3 days to induce shRNA expression, we found a significant reduction in HUWE1 protein and mRNA levels (Figure 10). No significant changes were observed in control cells or in cells transduced with HUWE1 shRNA but not treated with doxycycline suggesting this system has minimal leakage and is suitable HUWE1 suppression. To assess the specificity of primer pairs during qPCR analysis of mRNA levels of HUWE1 transcript, a melt-curve analysis was performed. A single peak was observed (data not shown) at °C for control primer, and °C for HUWE1 primer, indicating a single amplification product at the predicted Tp (Table 1).

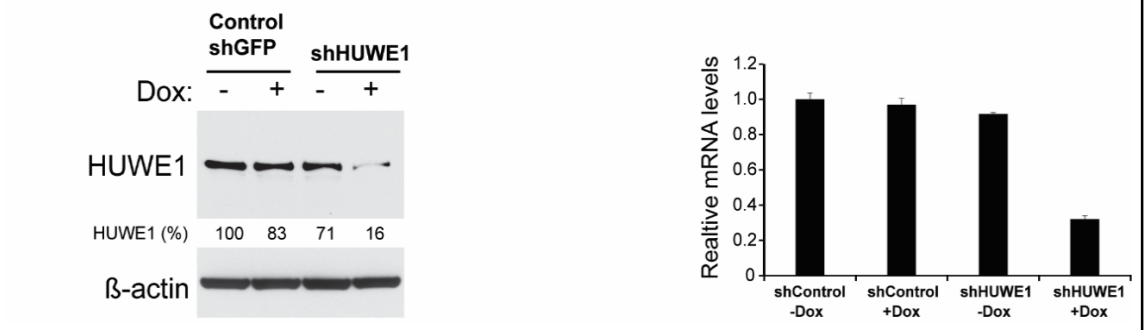

Figure 10. shRNA targeting HUWE1 suppresses protein and mRNA expression. **(**A) Western blot for HUWE1 in HCC827 cells expressing inducible shHUWE1 or control shGFP. shHUWE1 was induced by exposing cells to doxycycline (Dox)-containing media for 4 days. ß-actin was used as a loading control. (B)

Suppression of HUWE1 in *EGFR*-mutant lung cancer cells decreases dependence on EGFR in HCC827 cells.

To confirm if suppression of HUWE1 can modify dependence of mutant-EGFR signaling in response to erlotinib treatment, we constructed a shRNA targeting HUWE1 or a control shRNA targeting GFP in doxycycline-inducible expression vectors. We then infected HCC827 cells to generate stably transduced cell populations (TetOn-shHUWE1 or TetOn-shGFP). Consistent with the results obtained by the sgRNA screen performed by the Cheung lab, inducible shRNA-mediated suppression of HUWE1 in HCC827 cells increased cell viability in the presence of erlotinib treatment compared to cells cultured in the absence of doxycycline or cells expressing a control shGFP (Figure 11). Phosphorylated EGFR remained inhibited in cells that retained viability (Figure 17), indicating that failure of erlotinib to inhibit EGFR signaling was not contributing to the observed increase in cell viability.

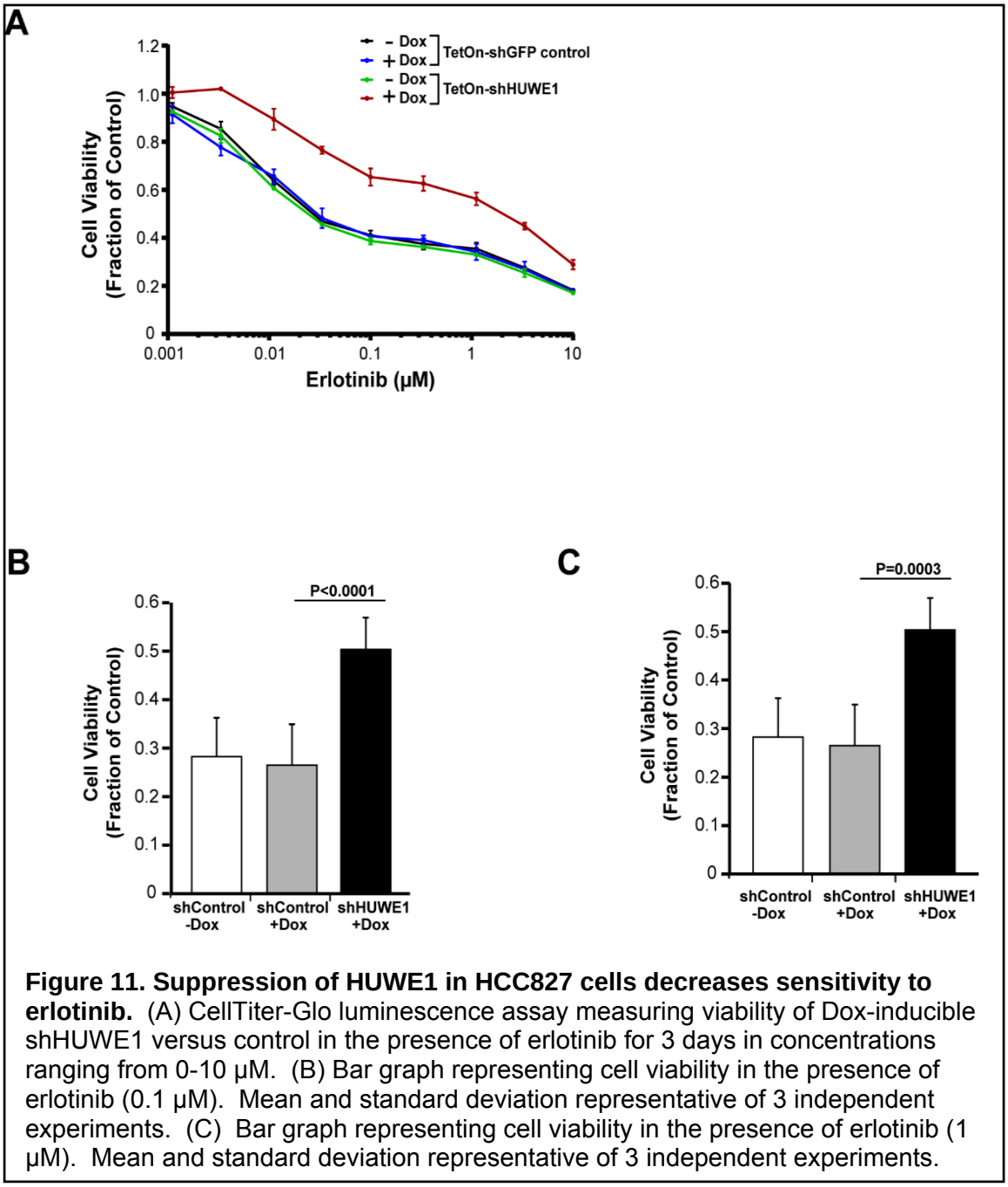

Figure 11. Suppression of HUWE1 in HCC827 cells decreases sensitivity to erlotinib. (A) CellTiter-Glo luminescence assay measuring viability of Dox-inducible shHUWE1 versus control in the presence of erlotinib for 3 days in concentrations ranging from 0-10 μM. (B) Bar graph representing cell viability in the presence of erlotinib (0.1 μM). Mean and standard deviation representative of 3 independent experiments. (C) Bar graph representing cell viability in the presence of erlotinib (1 μM). Mean and standard deviation representative of 3 independent experiments.

Suppression of HUWE1 increases tumor cell survival following exposure to EGFR-TKI

To further investigate whether increased cell viability that was observed was due to avoidance of apoptotic cell death or increased cell proliferation, we performed Annexin V staining on HCC827-shHUWE1 cells treated with erlotinib for 24 hours. We found that cells with suppressed HUWE1 expression had a significantly smaller population undergoing early-stage apoptosis (Annexin V-positive, propidium iodide-negative) than control cells (Figure 12). These results indicate that resistance was, at least in part, being mediated by decreased apoptosis and increased survival in HUWE1-suppressed cells.

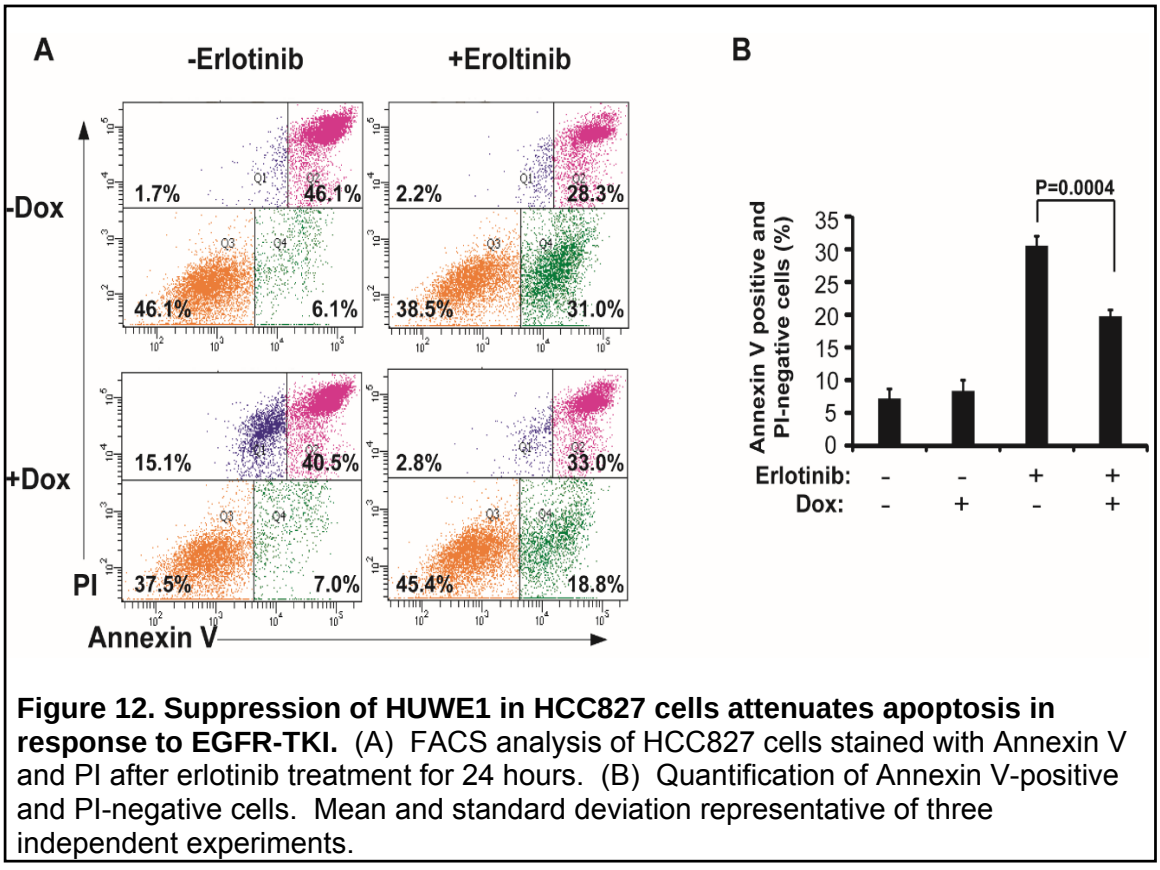

Figure 12. Suppression of HUWE1 in HCC827 cells attenuates apoptosis in response to EGFR-TKI. (A) FACS analysis of HCC827 cells stained with Annexin V and PI after erlotinib treatment for 24 hours. (B) Quantification of Annexin V-positive and PI-negative cells. Mean and standard deviation representative of three independent experiments.

HUWE1 suppression does not promote increased tumor cell proliferation upon EGFR-TKI

To investigate the effects of HUWE1 suppression on cell cycle, HCC827 cells were treated with erlotinib for 24 hours and stained with propidium iodide followed by FACS analysis. To determine the proliferative ability, HUWE1-suppressed cells were analyzed by FACS for BrdU uptake, an indicator of DNA synthesis. We found that suppression of HUWE1 did not affect cell cycle in response to erlotinib (Figure 13 A and B). However, erlotinib retained a dramatic effect on S phase regardless of whether HUWE1 was suppressed. We also found that HUWE1 suppression did not affect proliferative ability of the cells as there was no significant difference in BrdU uptake, a measure of DNA synthesis (Figure 13 C and D). Taken together, these data suggest that suppression of HUWE1 confers an erlotinib-resistant phenotype that is not mediated by alterations in cell cycle fractions.

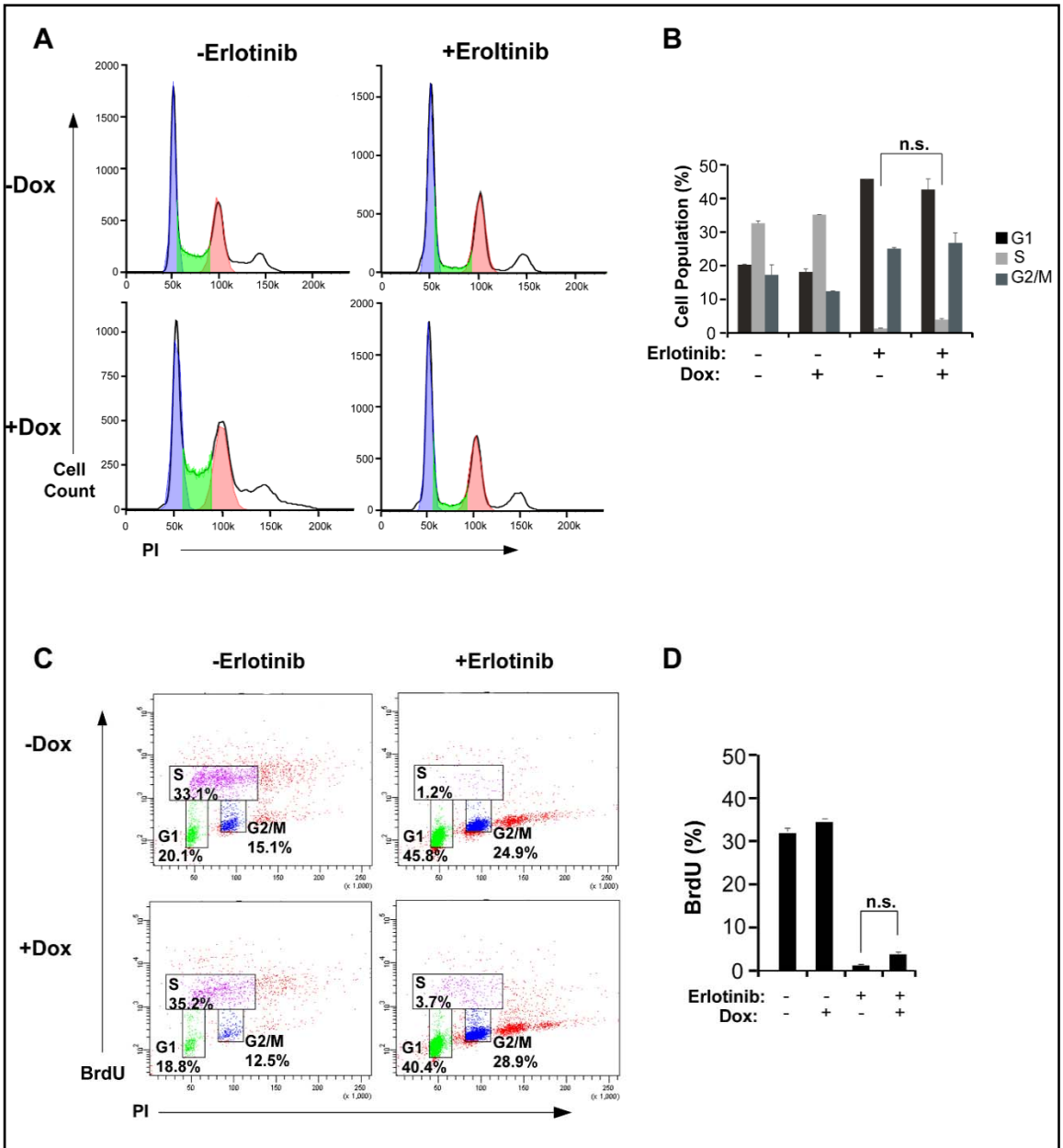

Figure 13. Suppression of HUWE1 in HCC827 cells does not affect cell cycle or proliferative ability in response to erlotinib. (A) FACS analysis of cell cycle populations in HCC827 cells after erlotinib treatment for 24 hours. (B) Quantification of cell populations (%). Mean and standard deviation representative of three independent experiments. (C) FACS analysis of BrdU incorporation after erlotinib treatment for 24 hours. (D) Quantification of BrdU-positive cell population. Mean and standard deviation representative of three independent experiments.

Suppression of HUWE1 in *EGFR*-mutant lung cancer cells promotes tumor cell survival upon EGFR inhibition through reactivation of AKT and ERK1/2 signaling

To determine whether suppression of HUWE1 in HCC827 cells affected activities of AKT and ERK1/2 signaling upon erlotinib treatment, we cultured HCC827-TetOn-shHUWE1 cells in the presence or absence of doxycycline for 4 days. Then we exposed them to different concentrations of erlotinib (0, 0.1, 1, and 10 μM) for 6 hours for immunoblot analyses. We found that phosphorylation of EGFR was similarly reduced in cells with or without HUWE1 suppression (Figure 14) after exposure to erlotinib. This result indicates that erlotinib was continuing to inhibit EGFR signaling in these cells, suggesting that drug resistance is occurring via an alternative mechanism. However, increased levels of phosphorylated-AKT (S473) and phosphorylated-ERK1/2 were detected in cells with HUWE1 (+Dox) suppression in response to erlotinib treatment compared to cells without HUWE1 suppression (-Dox) (Figure 14). Taken together, these data suggest that suppression of HUWE1 reactivates AKT and ERK1/2 signaling to activate downstream survival pathways and, moreover, to partially relieve cells of their dependence on oncogenic EGFR signaling for continued survival.

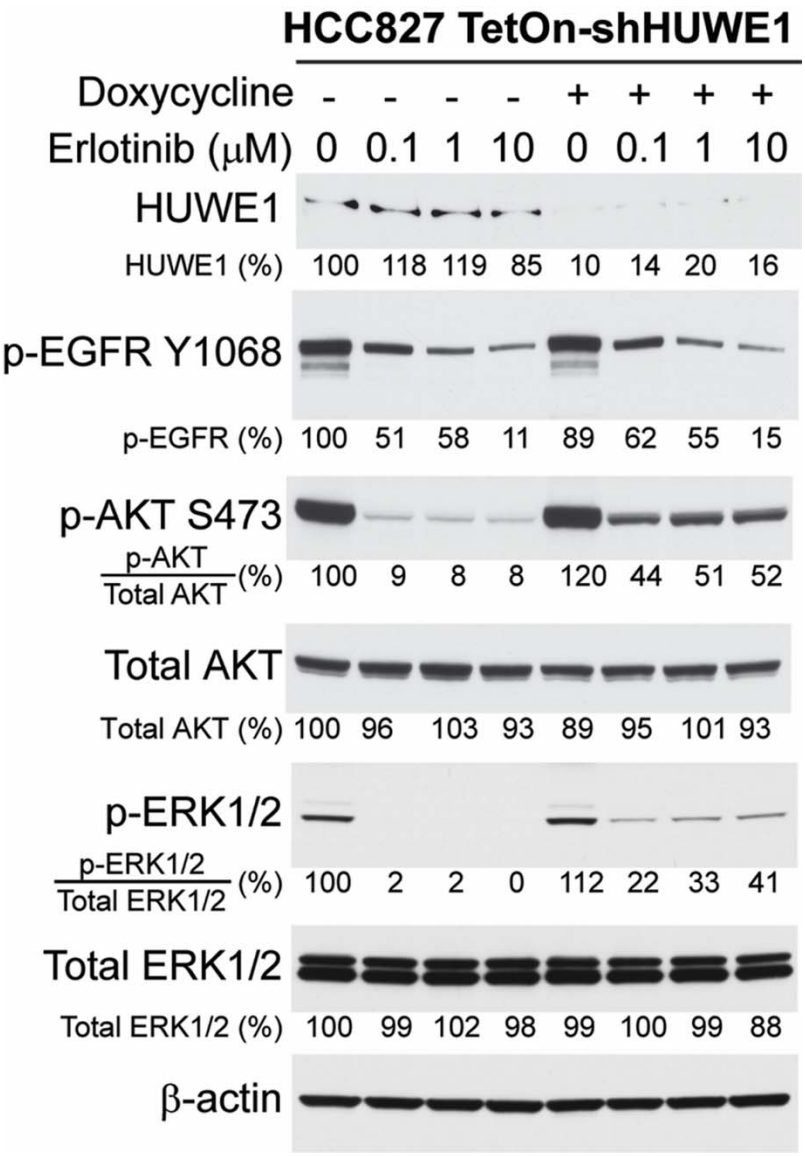

Figure 14. Suppression of HUWE1 in HCC827 cells reactivates AKT and ERK1/2 signaling despite the presence of EGFR inhibition. (A) Western blot for HUWE1 in HCC827 cells expressing inducible shHUWE1 or control shGFP. shHUWE1 was induced by exposing cells to doxycycline-containing media for 4 days then exposed to erlotinib for 6 hours in concentrations ranging from 0-10 μM. ß-actin was used as a loading control. Densitometry quantification relative to DMSO-treated in the absence of doxycycline.

Inhibition of PI3K or MEK suppresses EGFR inhibitor resistance induced by HUWE1 loss

To examine potential treatment strategies for EGFR inhibitor resistance induced by HUWE1 loss, we looked to restore EGFR inhibitor sensitivity by combination therapy with the PI3K inhibitor BEZ235 and the MEK inhibitor AZD6244. The restoration of EGFR-TKI sensitivity would indicate AKT and ERK1/2 signaling contribute to EGFR independence in HUWE1-suppressed cells. EGFR-mutant NSCLC cells were treated with erlotinib alone, erlotinib plus BEZ235, or erlotinib plus BEZ235 and AZD6244 for 72 hours. Relative viability was determined by measuring cellular ATP content. Combining erlotinib treatment with BEZ235 and AZD6244 in HUWE1-suppressed cells showed the greatest effect on cell viability, reducing the viability to a similar level seen in cells with uninhibited HUWE1 expression (Figure 15). These results suggest that increased AKT and ERK signaling mediates the observed EGFR independence induced by HUWE1 suppression.

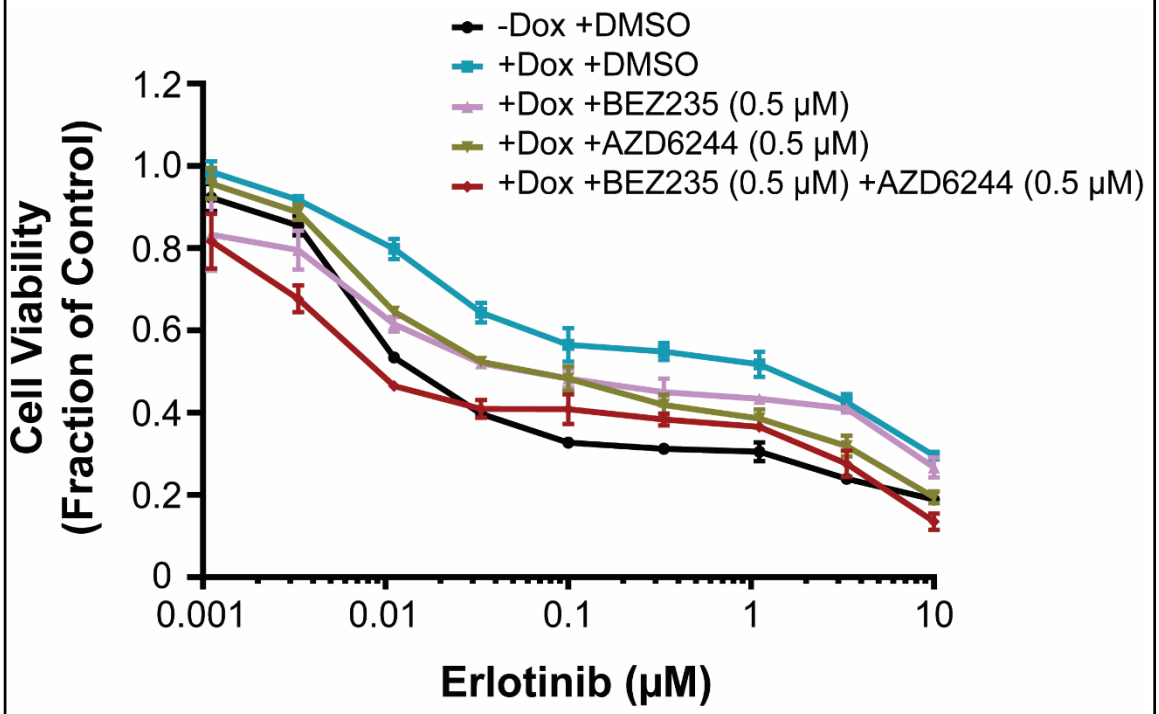

Figure 15. Inhibition of PI3K or MEK suppress HUWE1 loss-induced resistance to EGFR inhibitor. (A) CellTiter-Glo luminescence assay measuring proliferation of HCC827 cells expressing shHUWE1 in the presence of erlotinib alone, erlotinib and BEZ235, erlotinib and AZD6244, or erlotinib and BEZ235 and AZD 6244 versus non-induced shHUWE1 cells.

Suppression of HUWE1 increases ERK signaling in response to EGFR inhibition through stabilization of SHOC2

Previous studies have identified numerous candidate substrates that are directly regulated by HUWE1, such as SHOC2, RAF1, MCL1, and c-MYC. Therefore, we next investigated whether suppression of HUWE1 in HCC827 cells affected the levels of these substrates by immunoblot analyses. We found that suppression of HUWE1 led to increased protein levels of SHOC2 and c-Myc but did not affect the levels of RAF1 or MCL1 compared to cells with uninhibited HUWE1 expression (Figure 16). Induction of

BH3-only pro-apoptotic protein, specifically BIM, is necessary for erlotinib-mediated apoptosis, so we therefore wanted to know whether suppression of HUWE1 attenuates BIM induction in response to erlotinib. We found that suppression of HUWE1 led to decreased levels of BIM_{EL} in response to erlotinib treatment (Figure 16).

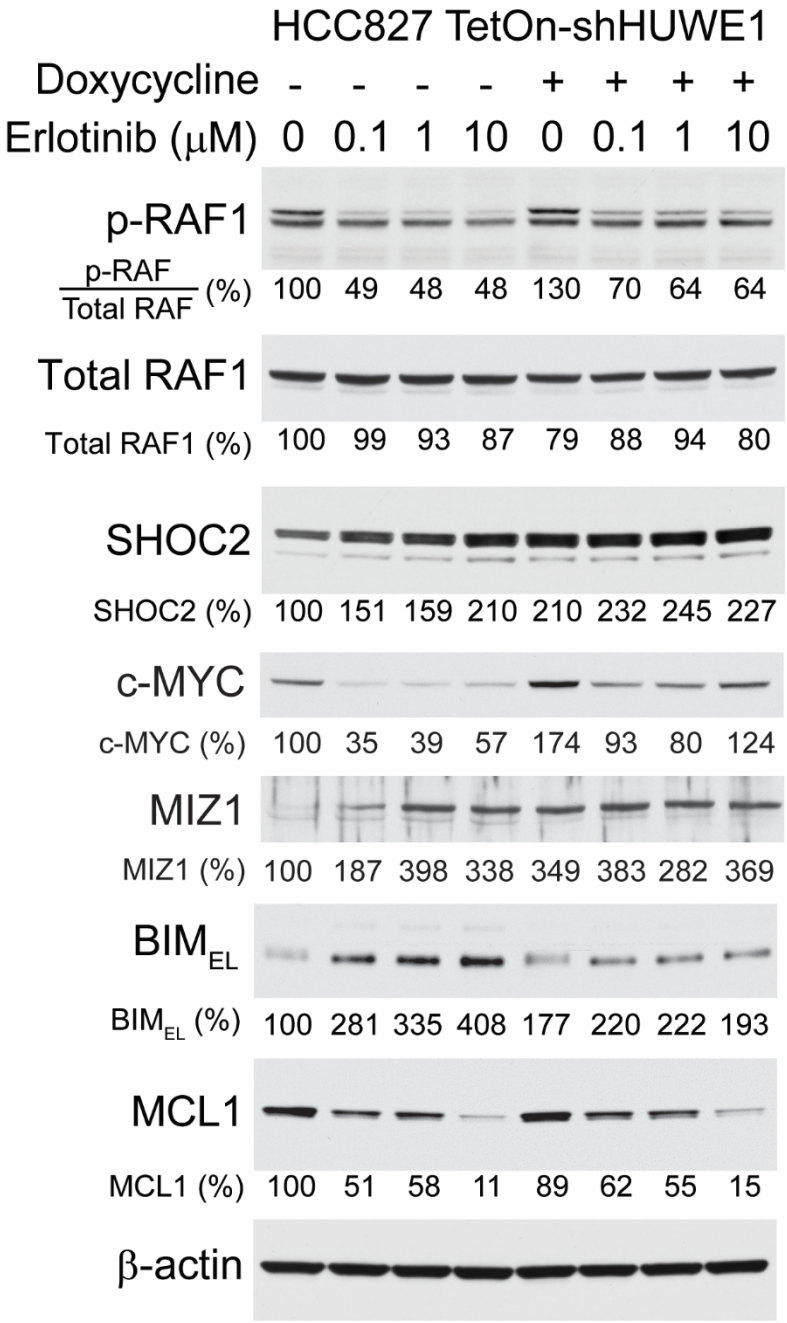

Figure 16. Suppression of HUWE1 in HCC827 cells increases SHOC2 and c-MYC levels and decreases BIM levels (A) Western blot for HUWE1 in HCC827 cells expressing inducible shHUWE1 or control shGFP. shHUWE1 was induced by exposing cells to doxycycline (Dox)-containing media for 4 days then exposed to erlotinib for 6 hours in concentrations ranging from 0-10 μM. ß-actin was used as a loading control. Densitometry quantification is relative to DMSO-treated in the absence of doxycycline.

Gene set enrichment analysis identifies differentially expressed transcripts in HUWE1-suppressed cells critical for EGFR-TKI response

To identify key genes critical to EGFR-TKI response whose expression may be altered upon erlotinib treatment when HUWE1 is suppressed, we performed gene set enrichment analysis on preliminary transcriptional profiling data performed by Dr. Cheung's laboratory. As expected, we found enrichment of a gene set that is downregulated by EGFR-TKI in sensitive EGFR-mutant NSCLC cells (Figure 17). This gene set was identified by the Kobayashi group when they used transcriptional profiling to determine genes whose down regulation is critical for EGFR-TKI sensitivity. Kobayashi et al., used H1975 cells which are EGFR-mutant but carry a T790M mutation rendering them insensitive to 1st generation EGFR-TKIs such as gefitinib due to ineffective drug binding. These cells were treated with DMSO, gefitinib or the irreversible EGFR inhibitor EKI-785 to which the cells are sensitive. Many of the genes highly down-regulated were factors regulated by EGFR signaling, those involved in a negative feedback loop of the MAPK pathway induced by oncogenic EGFR signaling, and activator protein-1 components such as c-Jun and FOS-like antigen1—mediators of MAPK and STAT signaling.

Of the 242 genes in this gene set, 157 are contained in the leading edge—those that contribute most to the enrichment. An enrichment heat map of these core genes are shown in Figure 18. These data suggest that HUWE1 suppression confers EGFR-TKI resistance by enriching the expression of genes whose down-regulation is critical for EGFR-TKI sensitivity.

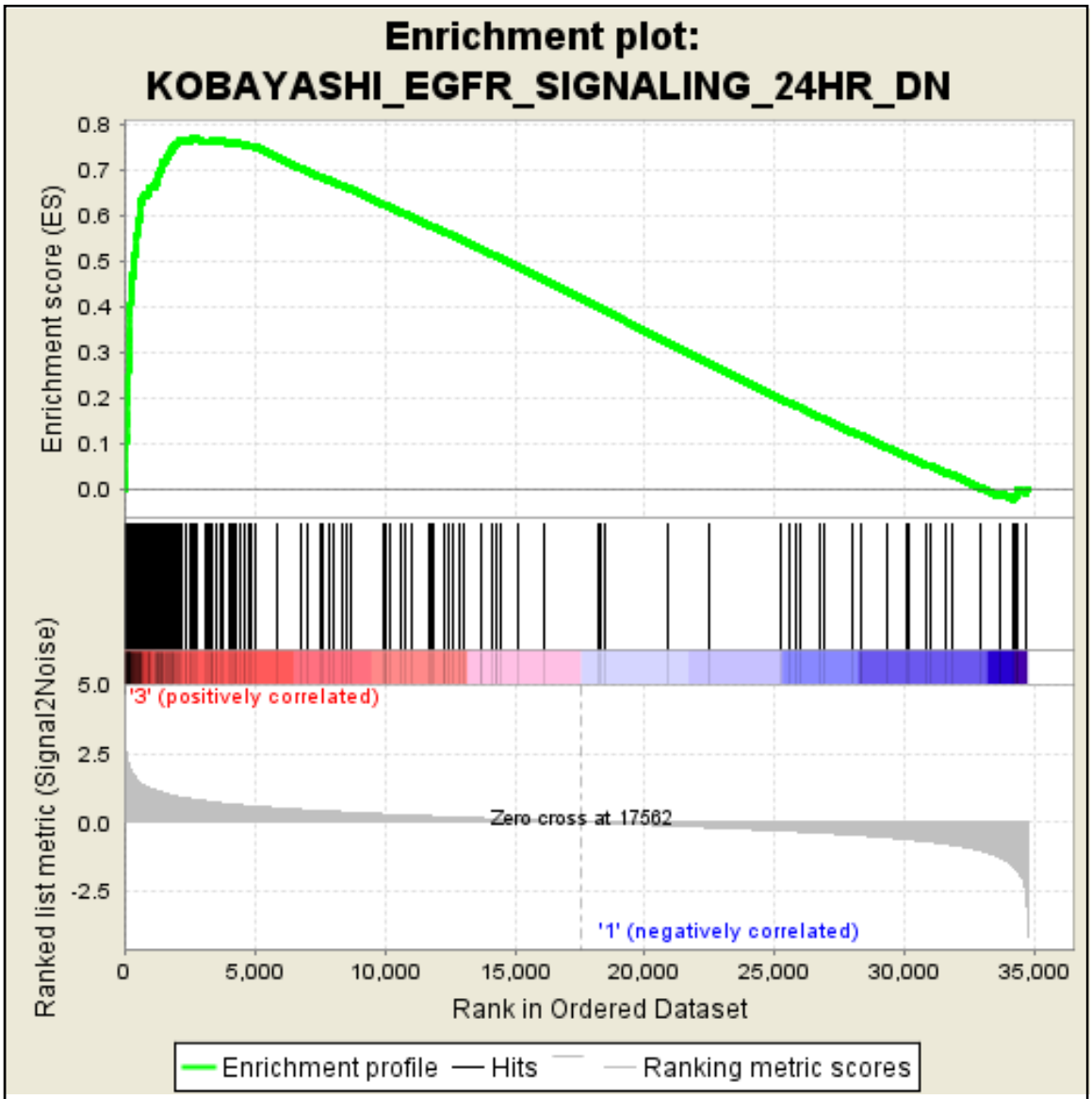

Figure 17. Kobayashi_EGFR_Signaling_24HR_DN Gene set enrichment analysis plot. Genes in this set are downregulated after 24 hour treatment with EGFR-TKI in EGFR-TKI-sensitive NSCLC cells. This plot represents enrichment of genes in HUWE1-suppressed HCC827 cells versus control cells using preliminary data obtained as previously described. P<0.0001; FDR Q<0.0001,

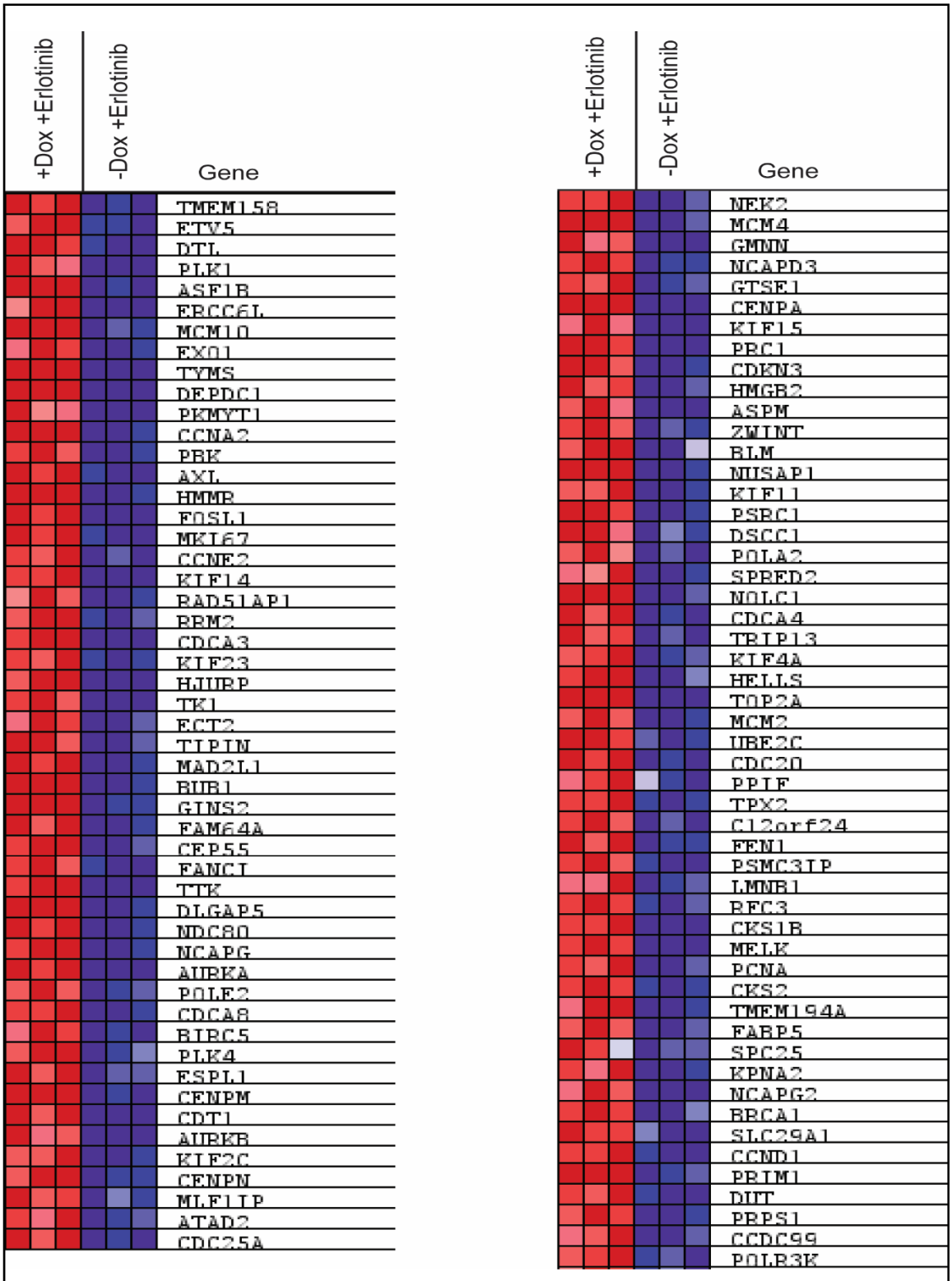

Figure 18. Core enrichment genes in Kobayashi_EGFR-Signaling_24HR_DN gene set. Enrichment heat map of core genes contributing to gene set enrichment. Each column indicative of independent experiment replicates.

Discussion and alternative approaches

In this aim, I showed that suppression of HUWE1 in NSCLC cells confers erlotinib resistance by reactivating ERK1/2 and AKT signaling pathways despite continued erlotinib exposure, allowing the cancer cells to escape apoptotic cell death. Combined inhibition of EGFR, ERK1/2 and AKT partially reversed resistance in HUWE1-suppressed cells and reduced cell viability to levels similar to control cells. This suggests that increased AKT and ERK1/2 signaling mediates the observed EGFR independence induced by HUWE1 suppression.

Cells with suppressed HUWE1 expression in the presence of erlotinib had higher viability compared to control cells and had significantly fewer cells in early apoptosis as determined by FACS analysis. There were no observed changes in cell cycle when HUWE1 was suppressed in response to erlotinib treatment, suggesting that reactivation of ERK1/2 and AKT mediated by HUWE1 suppression confers EGFR-TKI resistance by allowing tumor cells to escape erlotinib-induced apoptotic cell death.

Further investigation into how loss of HUWE1 mediates reactivation of ERK1/2 and AKT are warranted. One possible explanation is an increase in SHOC2 expression observed in shHUWE1-expressing cells. A known substrate of HUWE1, SHOC2, has been thought to accelerate the association of the RAS-RAF1 complex to regulate the ERK1/2 pathway [137].

We showed that after treatment with erlotinib, BIM induction was attenuated in HUWE1-suppressed cells compared to cells with uninhibited HUWE1 expression. Additional experiments should be performed to verify these results as well as to determine at what level BIM is regulated. For example, phosphorylation of BIM through

activation of ERK1/2 is sufficient for degradation of BIM_{EL}. However, BIM regulation may be mediated by other downstream kinases such as RSK1 [138], which is involved in cell survival.

We also showed that when HUWE1 is suppressed in HCC827 cells, there is an enrichment of expression of genes normally downregulated in response to EGFR-TKI in EGFR-mutant NSCLC. While we found a relatively large number of core differentially expressed genes enriched in response to erlotinib in HUWE1-suppressed cells that are down-regulated in sensitive cells, Cyclin D1 is particularly interesting. Cyclin D1 is a target of EGFR signaling whose expression is repressed upon erlotinib treatment in sensitive cells, and its down-regulation has been correlated with sensitivity to EGFR-TKIs [139]. Deletion of HUWE1 has been shown to repress MYC/MIZ1-mediated transcription of cyclin-dependent kinase inhibitor 2b [132], suggesting a possible mechanism of cyclin D1 enrichment.

For the experiments we performed, determination of cell viability relied on luminescent detection of ATP, an indicator of metabolic activity. While the experiments we performed were confirmed by triplicate experiments, there are several caveats worth mentioning when observing phenotypes by use of this assay. First, clear bottom plates were used, which makes for easier microscopic monitoring of cells through the duration of the experiment. However, it is possible to have increased signal crosstalk between wells. Additionally, if cells are plated at high density, contact growth inhibition may decrease cellular ATP, resulting in a non-linear relationship between luminescence value and cell number.

Advancements in CRISPR-mediated gene suppression employ a “nickase” Cas9 variant that generates a single- rather than a double-strand break to which the sgRNA

binds. By using paired sgRNAs to induce a double-strand break (one complementary to the sense strand and one complementary to the antisense strand), the probability of off-target binding within proximity to induce double-strand-break repair is low, thus reducing the off-target effects. Yet another CRISPR system seeks to further reduce off-target repair by fusing a Fok1 nuclease domain to a catalytically inactive Cas9. Again, double-strand breaks are achieved using paired sgRNAs. However, unlike Cas9, Fok1 must dimerize to generate a double-strand break [140]. Employing these CRISPR systems may be useful for increasing the specificity and thus improving the significance of observed phenotypes.

Specific Aim #2: **Assess the effects of HUWE1 suppression on tumor growth and survival in vivo.** A human xenograft mouse model was established to determine if suppression of HUWE1 affects tumor growth and survival in an in vivo setting. Validation of the sgRNA screen results in vitro indicated that HUWE1 can relieve EGFR-mutant NSCLC cells from their dependence on oncogenic EGFR signaling. Thus, the validation in vivo will support further studies of loss-of-HUWE1 as an EGFR-TKI resistance mechanism that may have clinical relevance.

Task #1: Establish HCC827-shHUWE1 xenografts in athymic nude mice and assess effects of HUWE1 suppression on tumor growth in response to erlotinib.

Task #2: Perform immunohistochemistry on tumor sections to visualize protein levels of p-AKT, p-ERK1/2, Ki67, and cleaved caspase-3.

Experimental Design

Cell culture: HCC827 cells were cultured in RPMI medium (Corning) supplemented with 10% fetal bovine serum (FBS; Corning) and 1× Penicillin-Streptomycin (Corning). Tetracycline-free FBS (Clontech) was used when tetracycline inducible expression system (TetOn) was applied. Packaging cells (293T) were cultured in DMEM medium (Corning) supplemented with 10% FBS (Corning).

Chemicals: Erlotinib was purchased from Selleck Chemicals and resuspended in 0.5% methylcellulose solution (Sigma).

Assessment of in vivo tumor growth in response to EGFR-TKI by xenograft: HCC827 cells stably transduced with pLKO-TetOn-shGFP or pLKO-TetOn-shHUWE1 were cultured as previously described. Cells were trypsinized, washed twice in 1× PBS, and resuspended in 1× PBS. In a volume of 200 µL of 1× PBS, 5×10^6 cells

were implanted subcutaneously into the left and right flanks of male athymic nude mice (Harlan Laboratories). Tumors were allowed to grow for 13 days before feeding mice with a normal diet or a doxycycline-containing diet (Harlan Laboratories). Starting from 17 days post implantation, tumor-bearing mice were either treated with erlotinib (25 mg/kg) once daily by oral garage or untreated. The size of tumors was measured by a digital caliper every 2 days.

$$\text{Tumor volume} = (\text{width})^2 \times \text{length}/2.$$

All tumors were fixed in 10% neutral buffered formalin for Hematoxylin and Eosin (H&E) staining and immunohistochemistry.

Immunohistochemistry: Formalin-fixed xenograft tumors were paraffin-embedded and sectioned (5 μm thick) by the Biorepository at the Medical University of South Carolina. Sectioned slides were prepared for immunohistochemistry by placing them in xylene 3 times for 5 minutes each time, 100% ethanol twice for 3 minutes each time, 95% ethanol once for 2 minutes, 80% ethanol once for 2 minutes, and 70% ethanol once for 5 minutes, followed by PBS for 5 minutes. Antigen retrieval was performed using the sodium citrate method by placing the slides into boiling sodium citrate (10 mM, pH 6) and microwaving them for 20 minutes at power level 5 (1200 watts). Endogenous peroxidase activity was blocked by incubating slides with 0.3% hydrogen peroxide (Sigma) in 1× PBS for 10 minutes and rinsed with distilled water (3 times for 5 minutes each) and PBS (once for 5 minutes).

To reduce background signal, sections were incubated with 2.5% goat serum blocking solution (Vector Labs) for 30 minutes. Blocking solution was removed and primary antibodies were immediately applied as follows: Cytokeratin 7 (1:100, Abcam);

Ki67 (1:100, Vector Labs); p-AKT Ser473 (1:100, Cell Signaling), p-ERK1/2 Thr202/Tyr204 (1:400, Cell Signaling) Cleaved caspase-3 (1:300, Cell Signaling). Slides were incubated overnight at 4°C. Slides were rinsed 3 times for 5 minutes each rinse in preparation for secondary antibody application. Biotinylated goat anti-rabbit or anti-mouse secondary antibodies were diluted (1:500) in 2.5% goat blocking serum in PBS. Appropriate secondary antibodies were added to slides and incubated for 1.5 hours. Primary antibodies were detected by using VECTASTAIN Elite ABC kit and DAB Peroxidase substrate kit (Vector Labs).

In preparation of primary antibody detection, slides were washed 3 times for 5 minutes each with PBS. ABC reagent was mixed according to manufacturer's instructions, applied to tissue sections, and incubated for 30 minutes. Slides were washed 3 times for 5 minutes each time with PBS. DAB reagent was prepared according to manufacturer's instructions and immediately applied to tissue sections after removal of ABC reagent. DAB reagent was incubated with slides until maximum color saturation was observed (2-10 minutes). Slides were then rinsed in distilled water for 5 minutes. Slides were counter-stained with hematoxylin (Vector Labs) for 1 minute and 45 seconds and rinsed with distilled water (2 times for 10 minutes each). Sections were dehydrated prior to applying coverslip by incubating in 75% ethanol for 5 minutes followed by 95% ethanol for 10 minutes, 100% ethanol for 10 minutes, and xylene (2 times for 10 minutes each). Representative images were taken using a Nikon DS-Fi1 camera.

Results

To examine the effects HUWE1 suppression on tumor growth upon erlotinib treatment in vivo, we used a doxycycline- inducible shRNA xenograft model in athymic nude mice. Mice were randomized and placed in 4 treatment groups: 1) No Dox, No erlotinib; 2) No Dox, Plus erlotinib; 3) Plus Dox, No erlotinib; and 4) Plus Dox, Plus erlotinib. HCC827 cells stably expressing inducible shHUWE1 were injected into the left and right flanks of the mice, and tumor development was monitored every other day by bilateral caliper measurement until average tumor diameter reached 10 mm. At that time, the tumors were excised, fixed, paraffin-embedded and sectioned. For the "Plus Dox" treatment groups, a doxycycline-containing diet was started 13 days after injection and continued for the duration of the experiment. Beginning 17 days after injection, erlotinib dosing was administered daily at 25 mg/kg by oral gavage, allowing time for induction of shHUWE1 expression after starting mice on doxycycline-containing diet (Figure 19).

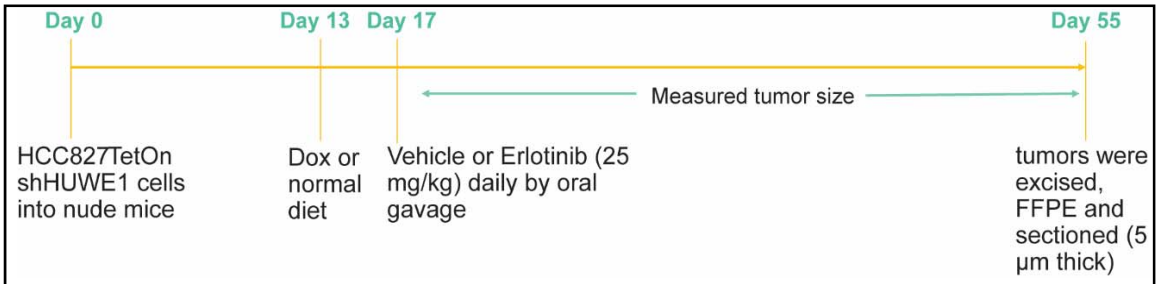

Figure 19. Timeline of xenograft experiment. HCC827 cells expressing inducible shHUWE1 implanted subcutaneously into the left and right flanks of athymic nude mice. After allowing tumors to grow for 13 days, mice were fed either normal or doxycycline-containing diet for the duration of the experiment. Erlotinib (25 mg/kg) was administered daily by oral gavage beginning on day 17 to allow for shHUWE1 to be induced. Upon initiation of erlotinib treatment, tumor volume was measured every other day using digital calipers. Mice were sacrificed when tumor size reached 1 cm in diameter. Tumors were then excised, formalin-fixed and paraffin-embedded, and sectioned.

We found that erlotinib treatment of mice that were fed with normal diet (-Dox) led to durable tumor regression throughout the treatment period. In contrast, mice fed with doxycycline-containing diet (+Dox) tumors regressed initially upon erlotinib treatment but continued to grow into large tumors ($n=5$, $P<0.0001$) (Figure 20 A). The tumors were excised at the end of the experiment and we found that the average of erlotinib-treated tumors with HUWE1 suppression were significantly heavier by weight than those with uninhibited HUWE1 expression ($P<0.0001$) (Figure 20 B). Taken together, these results show that suppression of HUWE1 in EGFR-mutant lung cancer cells decreased the dependence on EGFR for tumor growth in response to erlotinib treatment.

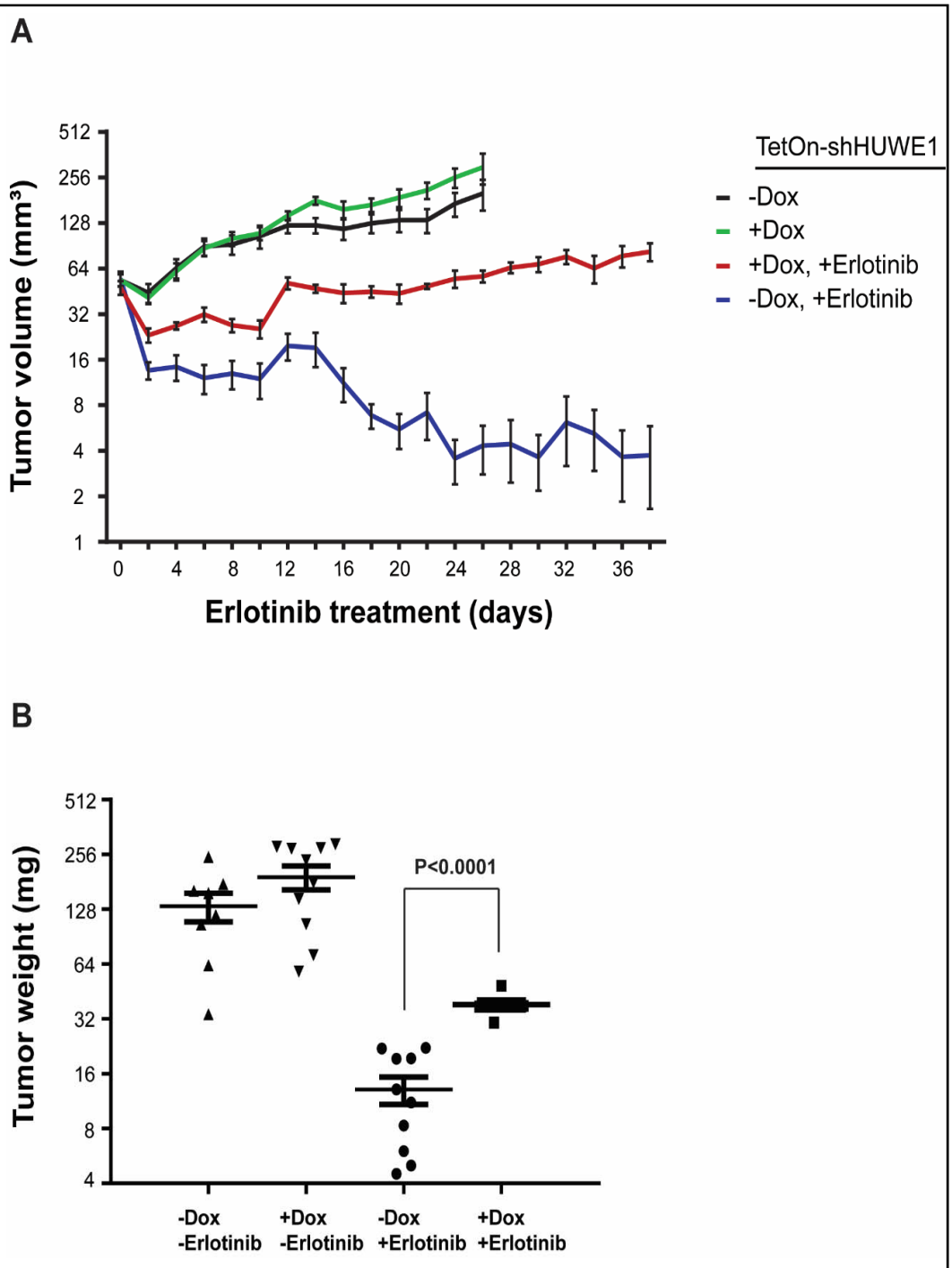

Figure 20. Suppression of HUWE1 increases tumor volume and weight after erlotinib treatment. (A) Tumor volume of murine xenografts (N=5) of subcutaneously implanted HCC827 cells expressing inducible shHUWE1. A doxycycline diet was administered 4 d prior to erlotinib treatment. Erlotinib was administered daily by oral gavage at a dosage of 25 mg/kg. (B) Scatter plot of tumor weight after excision.

To examine the effects HUWE1 suppression on AKT and ERK1/2 signaling in vivo, we performed immunohistochemistry on the tumor sections, staining for phosphorylated-AKT as well as phosphorylated-ERK1/2. In erlotinib-treated cells with HUWE1 suppression, we observed increased staining across both markers (Figure 21). This indicates HUWE1-suppression resulted in increased AKT and ERK1/2 signaling and suggests that the reactivation of these survival pathways contributed to the resistant phenotype. We also observed minimal differences in the untreated groups, confirming that the increased signaling is not a result of doxycycline alone.

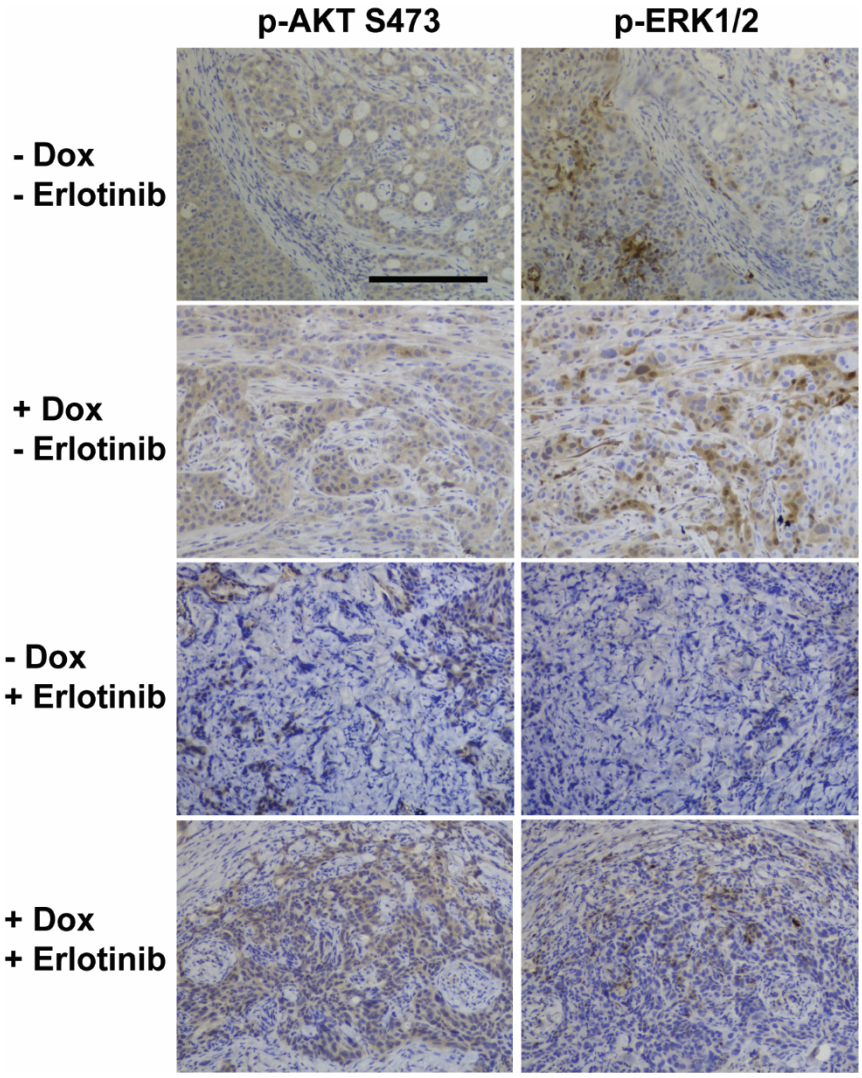

Figure 21. Suppression of HUWE1 in HCC827 xenografts reactivates AKT and ERK1/2 signaling in the presence of EGFR-TKI. Immunohistochemistry for p-AKT and p-ERK1/2 on tumors expressing Dox-inducible shHUWE1 implanted subcutaneously on left and right flanks of male athymic nude mice. After 13 days, mice were fed a Dox-containing diet for 3 days prior to erlotinib treatment. Mice were administered 25 mg/kg of erlotinib daily for 39 days.

Suppression of HUWE1 promotes EGFR-independent tumor growth by enhancing tumor cell proliferation and survival

To investigate the mechanisms by which suppression of HUWE1 promoted tumor growth upon erlotinib treatment, we performed immunohistochemistry on xenograft sections using antibodies against Ki67 and cleaved caspase-3 to analyze tumor cell proliferation and apoptosis, respectively. Staining for cytokeratin 7 was also performed to assist in identification of epithelial tumor cells. We found that erlotinib-treated tumors with uninhibited HUWE1 expression (-Dox, +Erlotinib) dramatically inhibited tumor cell proliferation and increased apoptotic cell death, whereas a relatively higher number of proliferating cells and lower number of apoptotic cells were detected in tumors in which HUWE1 was suppressed (+Dox, +Erlotinib) (Figure 22). These results suggest that suppression of HUWE1 promotes EGFR-independent tumor growth by enhancing tumor cell proliferation and survival.

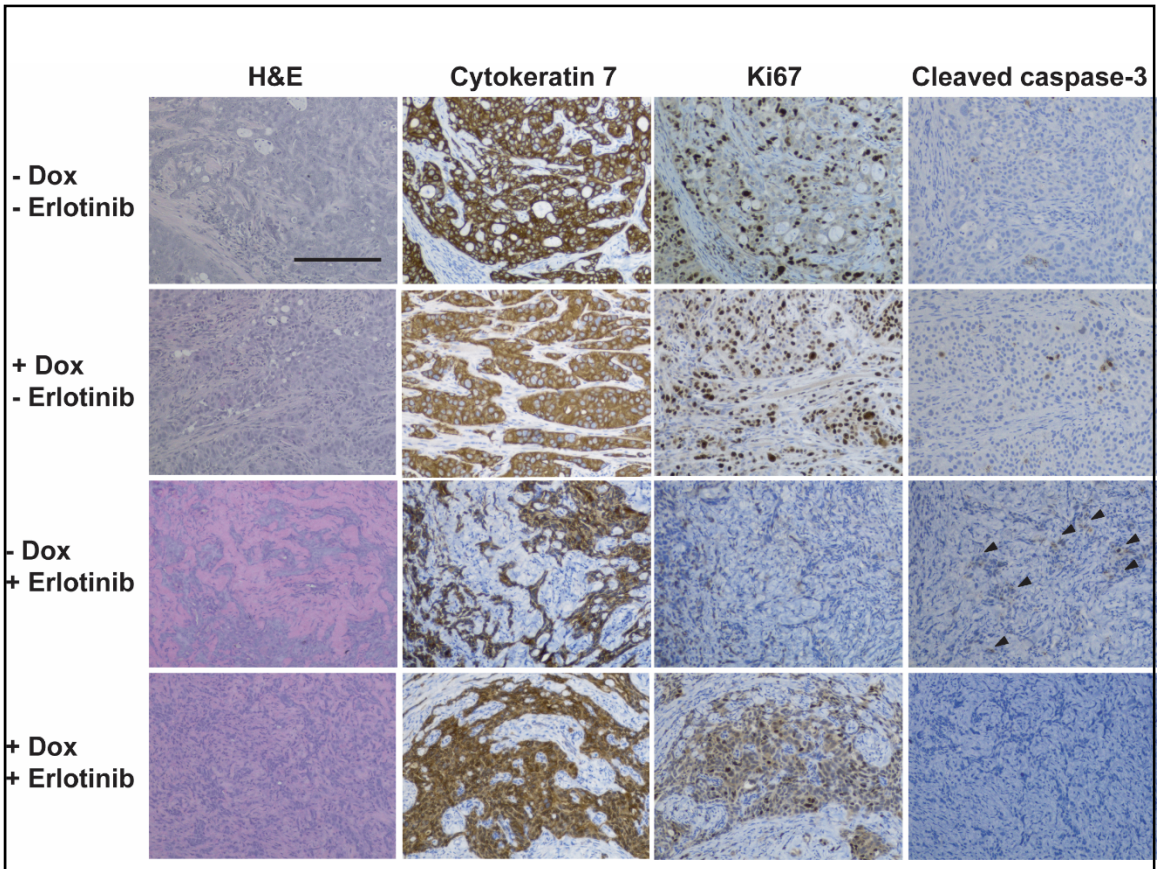

Figure 22. Suppression of HUWE1 in HCC827 xenografts increases proliferation and survival in response to EGFR-TKI. Immunohistochemistry for cytokeratin 7 and cleaved caspase-3 on tumors expressing Dox-inducible shHUWE1 implanted subcutaneously on left and right flanks of male athymic nude mice. After 13 days, mice were fed a Dox-containing diet for 3 days prior to erlotinib treatment. Mice were administered 25 mg/kg of erlotinib daily for 39 days.

Discussion and alternative approaches:

In this aim, I showed that suppression of HUWE1 in a human tumor xenograft model decreased the dependence on oncogenic EGFR signaling in EGFR-mutant lung cancer cells for tumor growth in response to erlotinib treatment.

Consistent with our in vitro results, we found by immunohistochemistry staining higher levels of phosphorylated-ERK1/2 and phosphorylated-AKT suggesting that these

signaling pathways may be involved in the increased tumor growth found in HUWE1-suppressed cells. Cleaved caspase-3 staining revealed that increased tumor growth is at least partially attributed to a decrease in tumor cells entering apoptosis upon erlotinib treatment. Interestingly, our in vivo data suggests that there is an increase in proliferation in these cells as well contrary to our in vivo data. One possible explanation is non-specific Ki67 staining, but further investigation is needed.

There are many variables that must be considered when conducting xenograft experiments. Site of implantation, agent formulation, dosing schedule, route of administration, and determination of experiment endpoint can all significantly affect outcome. Xenografts derived from cell lines undergo extensive selective pressures in culturing that may result in a more homogenous population than typically observed in patients. However, this relative homogeneity can be overcome by using xenografts derived directly from patient biopsies. Additionally, the surrounding tumor microenvironment—consisting of mainly fibroblasts, endothelial cells, and circulating immune cells—can impose selective conditions that greatly influence tumor growth and survival [141]. Thus, drug responses in xenograft models do not often correlate with patient responses in the clinic [142]. Despite this limitation, the results should not be discounted. Preclinical data obtained from human tumor xenografts have led to successful clinical trials. For example, HER2/neu-overexpressing human breast cancer xenografts led to the subsequent success of Herceptin combined with paclitaxel and doxorubicin to enhance anti-tumor activity in the clinic [143].

An alternative approach to overcome the limitations of the murine microenvironment is to partially reconstitute the human immune system to more accurately reflect the tumor microenvironment seen in human disease. Mice can be

"humanized" by direct injection of human peripheral blood [144] or implantation of human stromal tissue together with the tumor tissue [145]. Employing a humanized mouse model is expensive and technically challenging, and it should be noted that while humanized mice may help bridge the gap between human tumor tissue and the surrounding microenvironment, full restoration of HLA class I- and class II- selecting elements in T-cell populations remains a challenge [146].

Future Experiments

Validation of HUWE1 in additional cell lines and additional HUWE1-targeted shRNA

To improve our confidence that HUWE1 is a true modifier of EGFR dependence in EGFR-mutant NSCLC, I believe it is necessary to include additional cell lines in xenograft studies and determine whether the resistant phenotype is observed. To strengthen our observations further, additional shRNAs targeting HUWE1 should be employed.

Confirming the specificity of HUWE1-targeting shRNA

A caveat of shRNA-mediated gene suppression is the possibility that the observed phenotype is the result of off-target effects. Off-target effects can generally arise through complementarity of the shRNA sequence to unintended transcripts as well as saturation of the endogenous processing machinery, resulting in altered miRNA expression that could affect the observed phenotype. Well-designed shRNA sequences can mitigate off-target effects, but a critical step to show that direct HUWE1 suppression is mediating the observed phenotype is to ectopically express HUWE1 cDNA to rescue

the resistant phenotype. One method is to express cDNA of HUWE1 that contains a silent mutation in the region complementary to the shRNA target. By attaching an epitope tag, one can determine silencing of the endogenous protein but not the ectopic expression, as the epitope tag will cause a shift that can be identified by electrophoresis. An alternative approach would be to target the 3' untranslated region not present in the cDNA expression vector.

In the case of HUWE1, ectopic expression provides a specific challenge in that the open reading frame for HUWE1 is approximately 13kb, which can significantly limit lentiviral delivery due to low titers. Direct ordering of lentiviral particles is available, but due to the excessive cost, resource allocation needs to be considered. An alternative approach is to utilize the CRISPR/Cas9 system for gene activation. By fusing a catalytically inactive Cas9 fused to a transcriptional activator, we can target the HUWE1 promoter to activate gene transcription [147]. While shHUWE1 will target this transcript as well the increased expression may outcompete the ability of the shRNA-mediated suppression. This method of HUWE1 overexpression also has the added benefit of expression being driven by the endogenous promoter.

Targeting of additional bypass signaling tracks

Alternative kinase inhibitors targeting secondary EGFR mutations such as T790M are ineffective in the treatment of resistance mediated by the activation of parallel signaling pathways. A combination therapeutic approach is necessary in this setting. While this study focused on combined inhibition of EGFR with PI3K and MEK, other signaling pathways should be explored. STAT3 has been shown to be induced in response to erlotinib in EGFR-mutant NSCLC cell lines and associated with drug resistance [148, 149]. Niclosamide, an inhibitor of STAT3, has been shown to reverse

resistance in pooled populations of erlotinib-resistant populations of HCC827 cells [150]. Additionally, erlotinib and niclosamide work synergistically in the treatment of head and neck cancer [151]. While there may not be a direct relationship between HUWE1 and STAT3 signaling, the fate of cell survival is often a balance between pro- and anti-apoptotic signaling, and inhibition of erlotinib-mediated STAT3 induction in HUWE1-suppressed tumors may shift the balance to induce apoptosis and reverse resistance.

Clonogenic survival assay

To further characterize HUWE1-mediated cell death in response to EGFR-TKIs, clonogenic survival assays can determine the ability of a cell to retain its reproductive ability to form a large colony or clone. Removing the drug after an empirically determined time period has the added benefit of determining if the drug effect is irreversible.

HUWE1 substrate identification

While we have shown that suppression of HUWE1 reactivates AKT and ERK1/2 signaling to mediate EGFR-TKI resistance, little is known about how HUWE1 interacts with intermediate effectors involved to accomplish signal transduction. The identification of substrates targeted by HUWE1 in the context of EGFR inhibition is challenged by the often weak or transient interactions between E3 ligases and their substrates, making identification by immunoprecipitation and mass spectrometry difficult [152]. Ubiquitinated proteins may be rapidly degraded by the proteasome, and the use of proteasome inhibitors can have other biological consequences [153]. An emerging strategy to identify E3 ligase substrates is proximity-dependent biotin labeling in which an E3 protein is fused with a biotin-conjugating enzyme which reacts with nearby amine

groups on lysine residues. Interacting proteins can then be identified with semi-quantitative mass-spectrometry [154].

Analysis of patient tumor samples

The gold standard for tumor drug resistance studies is confirming candidate resistance effectors are relevant to cancer patients. Patient-matched tumor tissue obtained before treatment, and after tumor progression, should be analyzed for mechanistic characterization. Post-progression re-biopsies are often difficult to obtain due to the invasiveness of the procedure, and thus, acquiring a specimen collection that can provide significant insight presents a challenge.

Analysis of additional genes identified by CRISPR screen

The validity of the CRISPR/Cas9 knockout screen performed by the lab of Dr. Cheung was demonstrated by the identification of genes known to mediate EGFR-TKI resistance such as PTEN, NF1, NF2, TSC1, TSC2, and MED12. Furthermore, HUWE1, which has previously no known role in modifying EGFR dependence in EGFR-mutant NSCLC, was also validated by this study. This validity warrants further investigation of other novel genes identified by their screen, which could provide insights as to how these cells escape EGFR dependence upon EGFR inhibition. One such gene is inhibitor of kappa B-zeta (IκBζ), which has been shown to regulate NF-κB and STAT3 signaling [155, 156], both of which have been implicated in EGFR-TKI resistance [53, 148].

I believe this study provides the foundation to support HUWE1 as a modifier of EGFR dependence in EGFR-mutant NSCLC. However, numerous questions remain unanswered, and thus, further investigation is warranted. I believe the additional

aforementioned methods can provide mechanistic insight that could have clinical relevance.

Significance of study

Activating EGFR mutations in NSCLC have proven to be the Achilles' heel of these tumors, paving the way for the clinical success of EGFR-TKI inhibitors. Unfortunately, all patients who initially respond to this therapy will develop acquired resistance, demonstrating the persistent need to understand the underlying mechanisms involved. This need for understanding is truer now that we have seen several resistance mechanisms existing in patients synchronously or concurrently. To successfully overcome acquired EGFR-TKI resistance, combinational regimens will need to be explored. Overcoming acquired EGFR-TKI resistance requires the identification of genes that have the ability to allow tumor cells to escape their dependence on oncogenic EGFR signaling.

This study provides the first evidence showing that suppression of HUWE1 in EGFR-mutant lung cancer cells decreases dependence on EGFR signaling in response to EGFR inhibition. The underlying mechanisms involve the activation of both AKT and ERK1/2 signaling pathways.

References

1. Siegel, R.L., K.D. Miller, and A. Jemal, *Cancer statistics, 2016.* CA Cancer J Clin, 2016. **66**(1): p. 7-30.

2. National Center for Chronic Disease, P., S. Health Promotion Office on, and Health, *Reports of the Surgeon General*, in *The Health Consequences of Smoking-50 Years of Progress: A Report of the Surgeon General*. 2014, Centers for Disease Control and Prevention (US): Atlanta (GA).

3. *SEER Cancer Statistics Factsheets: Lung and Bronchus Cancer. Bethesda, MD: National Cancer Institute*. 2017 March 20, 2017]; Available from: https://seer.cancer.gov/statfacts/html/lungb.html.

4. Aberle, D.R., et al., *Reduced lung-cancer mortality with low-dose computed tomographic screening.* N Engl J Med, 2011. **365**(5): p. 395-409.

5. Fossella, F., et al., *Randomized, multinational, phase III study of docetaxel plus platinum combinations versus vinorelbine plus cisplatin for advanced non-small-cell lung cancer: the TAX 326 study group.* J Clin Oncol, 2003. **21**(16): p. 3016-24.

6. Azzoli, C.G., G. Giaccone, and S. Temin, *American Society of Clinical Oncology Clinical Practice Guideline Update on Chemotherapy for Stage IV Non-Small-Cell Lung Cancer.* J Oncol Pract, 2010. **6**(1): p. 39-43.

7. Weinstein, I.B., *Disorders in cell circuitry during multistage carcinogenesis: the role of homeostasis.* Carcinogenesis, 2000. **21**(5): p. 857-64.

8. Weinstein, I.B., *Cancer. Addiction to oncogenes--the Achilles heal of cancer.* Science, 2002. **297**(5578): p. 63-4.

9. Kantarjian, H., et al., *Hematologic and cytogenetic responses to imatinib mesylate in chronic myelogenous leukemia.* N Engl J Med, 2002. **346**(9): p. 645-52.

10. Pao, W., et al., *KRAS mutations and primary resistance of lung adenocarcinomas to gefitinib or erlotinib.* PLoS Med, 2005. **2**(1): p. e17.

11. Pao, W. and N. Girard, *New driver mutations in non-small-cell lung cancer.* Lancet Oncol, 2011. **12**(2): p. 175-80.

12. Normanno, N., et al., *Epidermal growth factor receptor (EGFR) signaling in cancer.* Gene, 2006. **366**(1): p. 2-16.

13. Carraway, K.L., 3rd, et al., *Neuregulin-2, a new ligand of ErbB3/ErbB4-receptor tyrosine kinases.* Nature, 1997. **387**(6632): p. 512-6.

14. Yarden, Y. and M.X. Sliwkowski, *Untangling the ErbB signalling network.* Nat Rev Mol Cell Biol, 2001. **2**(2): p. 127-37.

15. Olayioye, M.A., et al., *The ErbB signaling network: receptor heterodimerization in development and cancer.* Embo j, 2000. **19**(13): p. 3159-67.

16. Schlessinger, J., *Cell signaling by receptor tyrosine kinases.* Cell, 2000. **103**(2): p. 211-25.

17. Tzahar, E., et al., *A hierarchical network of interreceptor interactions determines signal transduction by Neu differentiation factor/neuregulin and epidermal growth factor.* Mol Cell Biol, 1996. **16**(10): p. 5276-87.

18. Guy, P.M., et al., *Insect cell-expressed p180erbB3 possesses an impaired tyrosine kinase activity.* Proc Natl Acad Sci U S A, 1994. **91**(17): p. 8132-6.

19. Jorissen, R.N., et al., *Epidermal growth factor receptor: mechanisms of activation and signalling.* Exp Cell Res, 2003. **284**(1): p. 31-53.

20. Olayioye, M.A., et al., *ErbB receptor-induced activation of stat transcription factors is mediated by Src tyrosine kinases.* J Biol Chem, 1999. **274**(24): p. 17209-18.

21. Pines, G., W.J. Kostler, and Y. Yarden, *Oncogenic mutant forms of EGFR: lessons in signal transduction and targets for cancer therapy.* FEBS Lett, 2010. **584**(12): p. 2699-706.

22. Landau, M. and N. Ben-Tal, *Dynamic equilibrium between multiple active and inactive conformations explains regulation and oncogenic mutations in ErbB receptors.* Biochim Biophys Acta, 2008. **1785**(1): p. 12-31.

23. Chen, Y.R., et al., *Distinctive activation patterns in constitutively active and gefitinib-sensitive EGFR mutants.* Oncogene, 2006. **25**(8): p. 1205-15.

24. Politi, K. and T.J. Lynch, *Two sides of the same coin: EGFR exon 19 deletions and insertions in lung cancer.* Clin Cancer Res, 2012. **18**(6): p. 1490-2.

25. Yun, C.H., et al., *Structures of lung cancer-derived EGFR mutants and inhibitor complexes: mechanism of activation and insights into differential inhibitor sensitivity.* Cancer Cell, 2007. **11**(3): p. 217-27.

26. Chung, C., *Tyrosine kinase inhibitors for epidermal growth factor receptor gene mutation-positive non-small cell lung cancers: an update for recent advances in therapeutics.* J Oncol Pharm Pract, 2016. **22**(3): p. 461-76.

27. Paez, J.G., et al., *EGFR mutations in lung cancer: correlation with clinical response to gefitinib therapy.* Science, 2004. **304**(5676): p. 1497-500.

28. Pao, W., et al., *EGF receptor gene mutations are common in lung cancers from "never smokers" and are associated with sensitivity of tumors to gefitinib and erlotinib.* Proc Natl Acad Sci U S A, 2004. **101**(36): p. 13306-11.

29. Mukohara, T., et al., *Differential effects of gefitinib and cetuximab on non-small-cell lung cancers bearing epidermal growth factor receptor mutations.* J Natl Cancer Inst, 2005. **97**(16): p. 1185-94.

30. Greulich, H., et al., *Oncogenic transformation by inhibitor-sensitive and -resistant EGFR mutants.* PLoS Med, 2005. **2**(11): p. e313.

31. Rosell, R., et al., *Erlotinib versus standard chemotherapy as first-line treatment for European patients with advanced EGFR mutation-positive non-small-cell lung cancer (EURTAC): a multicentre, open-label, randomised phase 3 trial.* Lancet Oncol, 2012. **13**(3): p. 239-46.

32. Mitsudomi, T., et al., *Gefitinib versus cisplatin plus docetaxel in patients with non-small-cell lung cancer harbouring mutations of the epidermal growth*

factor receptor (WJTOG3405): an open label, randomised phase 3 trial. Lancet Oncol, 2010. **11**(2): p. 121-8.

33. Maemondo, M., et al., *Gefitinib or chemotherapy for non-small-cell lung cancer with mutated EGFR.* N Engl J Med, 2010. **362**(25): p. 2380-8.

34. Yang, C.H., et al., *Specific EGFR mutations predict treatment outcome of stage IIIB/IV patients with chemotherapy-naive non-small-cell lung cancer receiving first-line gefitinib monotherapy.* J Clin Oncol, 2008. **26**(16): p. 2745-53.

35. Yun, C.H., et al., *The T790M mutation in EGFR kinase causes drug resistance by increasing the affinity for ATP.* Proc Natl Acad Sci U S A, 2008. **105**(6): p. 2070-5.

36. Sequist, L.V., et al., *First-line gefitinib in patients with advanced non-small-cell lung cancer harboring somatic EGFR mutations.* J Clin Oncol, 2008. **26**(15): p. 2442-9.

37. Inoue, A., et al., *Prospective phase II study of gefitinib for chemotherapy-naive patients with advanced non-small-cell lung cancer with epidermal growth factor receptor gene mutations.* J Clin Oncol, 2006. **24**(21): p. 3340-6.

38. Asahina, H., et al., *A phase II trial of gefitinib as first-line therapy for advanced non-small cell lung cancer with epidermal growth factor receptor mutations.* Br J Cancer, 2006. **95**(8): p. 998-1004.

39. Mok, T.S., et al., *Gefitinib or carboplatin-paclitaxel in pulmonary adenocarcinoma.* N Engl J Med, 2009. **361**(10): p. 947-57.

40. Zhou, C., et al., *Erlotinib versus chemotherapy as first-line treatment for patients with advanced EGFR mutation-positive non-small-cell lung cancer (OPTIMAL, CTONG-0802): a multicentre, open-label, randomised, phase 3 study.* Lancet Oncol, 2011. **12**(8): p. 735-42.

41. Jackman, D.M., et al., *Exon 19 deletion mutations of epidermal growth factor receptor are associated with prolonged survival in non-small cell lung cancer patients treated with gefitinib or erlotinib.* Clin Cancer Res, 2006. **12**(13): p. 3908-14.

42. Taron, M., et al., *Activating mutations in the tyrosine kinase domain of the epidermal growth factor receptor are associated with improved survival in gefitinib-treated chemorefractory lung adenocarcinomas.* Clin Cancer Res, 2005. **11**(16): p. 5878-85.

43. Han, S.W., et al., *Predictive and prognostic impact of epidermal growth factor receptor mutation in non-small-cell lung cancer patients treated with gefitinib.* J Clin Oncol, 2005. **23**(11): p. 2493-501.

44. Kiyohara, Y., N. Yamazaki, and A. Kishi, *Erlotinib-related skin toxicities: treatment strategies in patients with metastatic non-small cell lung cancer.* J Am Acad Dermatol, 2013. **69**(3): p. 463-72.

45. Harandi, A., et al., *Clinical Efficacy and Toxicity of Anti-EGFR Therapy in Common Cancers.* J Oncol, 2009. **2009**: p. 567486.

46. Jackman, D., et al., *Clinical definition of acquired resistance to epidermal growth factor receptor tyrosine kinase inhibitors in non-small-cell lung cancer.* J Clin Oncol, 2010. **28**(2): p. 357-60.

47. Yu, H.A., et al., *Analysis of tumor specimens at the time of acquired resistance to EGFR-TKI therapy in 155 patients with EGFR-mutant lung cancers.* Clin Cancer Res, 2013. **19**(8): p. 2240-7.

48. Kobayashi, S., et al., *EGFR mutation and resistance of non-small-cell lung cancer to gefitinib.* N Engl J Med, 2005. **352**(8): p. 786-92.

49. Pao, W., et al., *Acquired resistance of lung adenocarcinomas to gefitinib or erlotinib is associated with a second mutation in the EGFR kinase domain.* PLoS Med, 2005. **2**(3): p. e73.

50. Engelman, J.A., et al., *MET amplification leads to gefitinib resistance in lung cancer by activating ERBB3 signaling.* Science, 2007. **316**(5827): p. 1039-43.

51. Yano, S., et al., *Ligand-triggered resistance to molecular targeted drugs in lung cancer: roles of hepatocyte growth factor and epidermal growth factor receptor ligands.* Cancer Sci, 2012. **103**(7): p. 1189-94.

52. Cheung, H.W., et al., *Amplification of CRKL induces transformation and epidermal growth factor receptor inhibitor resistance in human non-small cell lung cancers.* Cancer Discov, 2011. **1**(7): p. 608-25.

53. Bivona, T.G., et al., *FAS and NF-kappaB signalling modulate dependence of lung cancers on mutant EGFR.* Nature, 2011. **471**(7339): p. 523-6.

54. Sequist, L.V., et al., *Genotypic and histological evolution of lung cancers acquiring resistance to EGFR inhibitors.* Sci Transl Med, 2011. **3**(75): p. 75ra26.

55. Ohashi, K., et al., *Lung cancers with acquired resistance to EGFR inhibitors occasionally harbor BRAF gene mutations but lack mutations in KRAS, NRAS, or MEK1.* Proc Natl Acad Sci U S A, 2012. **109**(31): p. E2127-33.

56. Takezawa, K., et al., *HER2 amplification: a potential mechanism of acquired resistance to EGFR inhibition in EGFR-mutant lung cancers that lack the second-site EGFRT790M mutation.* Cancer Discov, 2012. **2**(10): p. 922-33.

57. Gong, Y., et al., *Induction of BIM is essential for apoptosis triggered by EGFR kinase inhibitors in mutant EGFR-dependent lung adenocarcinomas.* PLoS Med, 2007. **4**(10): p. e294.

58. Faber, A.C., et al., *BIM expression in treatment-naive cancers predicts responsiveness to kinase inhibitors.* Cancer Discov, 2011. **1**(4): p. 352-65.

59. Lee, J.Y., et al., *The BIM Deletion Polymorphism and its Clinical Implication in Patients with EGFR-Mutant Non-Small-Cell Lung Cancer Treated with EGFR Tyrosine Kinase Inhibitors.* J Thorac Oncol, 2015. **10**(6): p. 903-9.

60. Kang, Y. and J. Massague, *Epithelial-mesenchymal transitions: twist in development and metastasis.* Cell, 2004. **118**(3): p. 277-9.

61. Uramoto, H., et al., *Expression of selected gene for acquired drug resistance to EGFR-TKI in lung adenocarcinoma.* Lung Cancer, 2011. **73**(3): p. 361-5.

62. Hrustanovic, G., B.J. Lee, and T.G. Bivona, *Mechanisms of resistance to EGFR targeted therapies.* Cancer Biol Ther, 2013. **14**(4): p. 304-14.

63. Katada, T., et al., *Synergistic activation of a family of phosphoinositide 3-kinase via G-protein coupled and tyrosine kinase-related receptors.* Chem Phys Lipids, 1999. **98**(1-2): p. 79-86.

64. Liu, P., Z. Wang, and W. Wei, *Phosphorylation of Akt at the C-terminal tail triggers Akt activation.* Cell Cycle, 2014. **13**(14): p. 2162-4.

65. Sakai, A., et al., *PTEN gene alterations in lymphoid neoplasms.* Blood, 1998. **92**(9): p. 3410-5.

66. Taylor, V., et al., *5' phospholipid phosphatase SHIP-2 causes protein kinase B inactivation and cell cycle arrest in glioblastoma cells.* Mol Cell Biol, 2000. **20**(18): p. 6860-71.

67. Vazquez, F. and W.R. Sellers, *The PTEN tumor suppressor protein: an antagonist of phosphoinositide 3-kinase signaling.* Biochim Biophys Acta, 2000. **1470**(1): p. M21-35.

68. Meyer, D.S., et al., *Expression of PIK3CA mutant E545K in the mammary gland induces heterogeneous tumors but is less potent than mutant H1047R.* Oncogenesis, 2013. **2**: p. e74.

69. Nicholson, K.M. and N.G. Anderson, *The protein kinase B/Akt signalling pathway in human malignancy.* Cell Signal, 2002. **14**(5): p. 381-95.

70. Cseh, B., E. Doma, and M. Baccarini, *"RAF" neighborhood: protein-protein interaction in the Raf/Mek/Erk pathway.* FEBS Lett, 2014. **588**(15): p. 2398-406.

71. Li, W., M. Han, and K.L. Guan, *The leucine-rich repeat protein SUR-8 enhances MAP kinase activation and forms a complex with Ras and Raf.* Genes Dev, 2000. **14**(8): p. 895-900.

72. Jang, E.R., et al., *HUWE1 is a molecular link controlling RAF-1 activity supported by the Shoc2 scaffold.* Mol Cell Biol, 2014. **34**(19): p. 3579-93.

73. Pulverer, B.J., et al., *Phosphorylation of c-jun mediated by MAP kinases.* Nature, 1991. **353**(6345): p. 670-4.

74. Yang, B.S., et al., *Ras-mediated phosphorylation of a conserved threonine residue enhances the transactivation activities of c-Ets1 and c-Ets2.* Mol Cell Biol, 1996. **16**(2): p. 538-47.

75. Gupta, S. and R.J. Davis, *MAP kinase binds to the NH2-terminal activation domain of c-Myc.* FEBS Lett, 1994. **353**(3): p. 281-5.

76. Blenis, J., *Signal transduction via the MAP kinases: proceed at your own RSK.* Proc Natl Acad Sci U S A, 1993. **90**(13): p. 5889-92.

77. Norris, J.L. and A.S. Baldwin, Jr., *Oncogenic Ras enhances NF-kappaB transcriptional activity through Raf-dependent and Raf-independent mitogen-activated protein kinase signaling pathways.* J Biol Chem, 1999. **274**(20): p. 13841-6.

78. O'Connor, L., et al., *Bim: a novel member of the Bcl-2 family that promotes apoptosis.* Embo j, 1998. **17**(2): p. 384-95.

79. Westphal, D., R.M. Kluck, and G. Dewson, *Building blocks of the apoptotic pore: how Bax and Bak are activated and oligomerize during apoptosis.* Cell Death Differ, 2014. **21**(2): p. 196-205.

80. Willis, S.N. and J.M. Adams, *Life in the balance: how BH3-only proteins induce apoptosis.* Curr Opin Cell Biol, 2005. **17**(6): p. 617-25.

81. Zhong, Q., et al., *Mule/ARF-BP1, a BH3-only E3 ubiquitin ligase, catalyzes the polyubiquitination of Mcl-1 and regulates apoptosis.* Cell, 2005. **121**(7): p. 1085-95.

82. Inuzuka, H., et al., *SCF(FBW7) regulates cellular apoptosis by targeting MCL1 for ubiquitylation and destruction.* Nature, 2011. **471**(7336): p. 104-9.

83. Luciano, F., et al., *Phosphorylation of Bim-EL by Erk1/2 on serine 69 promotes its degradation via the proteasome pathway and regulates its proapoptotic function.* Oncogene, 2003. **22**(43): p. 6785-93.

84. Dijkers, P.F., et al., *Expression of the pro-apoptotic Bcl-2 family member Bim is regulated by the forkhead transcription factor FKHR-L1.* Curr Biol, 2000. **10**(19): p. 1201-4.

85. Ley, R., et al., *Activation of the ERK1/2 signaling pathway promotes phosphorylation and proteasome-dependent degradation of the BH3-only protein, Bim.* J Biol Chem, 2003. **278**(21): p. 18811-6.

86. Tzivion, G., M. Dobson, and G. Ramakrishnan, *FoxO transcription factors; Regulation by AKT and 14-3-3 proteins.* Biochim Biophys Acta, 2011. **1813**(11): p. 1938-45.

87. Karachaliou, N., et al., *BIM and mTOR expression levels predict outcome to erlotinib in EGFR-mutant non-small-cell lung cancer.* Sci Rep, 2015. **5**: p. 17499.

88. Costa, D.B., et al., *BIM mediates EGFR tyrosine kinase inhibitor-induced apoptosis in lung cancers with oncogenic EGFR mutations.* PLoS Med, 2007. **4**(10): p. 1669-79; discussion 1680.

89. Cragg, M.S., et al., *Gefitinib-induced killing of NSCLC cell lines expressing mutant EGFR requires BIM and can be enhanced by BH3 mimetics.* PLoS Med, 2007. **4**(10): p. 1681-89; discussion 1690.

90. Zhao, M., et al., *The Bim deletion polymorphism clinical profile and its relation with tyrosine kinase inhibitor resistance in Chinese patients with non-small cell lung cancer.* Cancer, 2014. **120**(15): p. 2299-307.

91. Hershko, A. and A. Ciechanover, *The ubiquitin system.* Annu Rev Biochem, 1998. **67**: p. 425-79.

92. Sigismund, S., S. Polo, and P.P. Di Fiore, *Signaling through monoubiquitination.* Curr Top Microbiol Immunol, 2004. **286**: p. 149-85.

93. Mukhopadhyay, D. and H. Riezman, *Proteasome-independent functions of ubiquitin in endocytosis and signaling.* Science, 2007. **315**(5809): p. 201-5.

94. Berndsen, C.E. and C. Wolberger, *New insights into ubiquitin E3 ligase mechanism.* 2014. **21**(4): p. 301-7.

95. Maheswaran, S., et al., *Detection of mutations in EGFR in circulating lung-cancer cells.* N Engl J Med, 2008. **359**(4): p. 366-77.

96. Nguyen, K.S., S. Kobayashi, and D.B. Costa, *Acquired resistance to epidermal growth factor receptor tyrosine kinase inhibitors in non-small-cell lung cancers dependent on the epidermal growth factor receptor pathway.* Clin Lung Cancer, 2009. **10**(4): p. 281-9.

97. Li, D., et al., *BIBW2992, an irreversible EGFR/HER2 inhibitor highly effective in preclinical lung cancer models.* Oncogene, 2008. **27**(34): p. 4702-11.

98. Kwak, E.L., et al., *Irreversible inhibitors of the EGF receptor may circumvent acquired resistance to gefitinib.* Proc Natl Acad Sci U S A, 2005. **102**(21): p. 7665-70.

99. Engelman, J.A., et al., *PF00299804, an irreversible pan-ERBB inhibitor, is effective in lung cancer models with EGFR and ERBB2 mutations that are resistant to gefitinib.* Cancer Res, 2007. **67**(24): p. 11924-32.

100. Sequist, L.V., et al., *Neratinib, an irreversible pan-ErbB receptor tyrosine kinase inhibitor: results of a phase II trial in patients with advanced non-small-cell lung cancer.* J Clin Oncol, 2010. **28**(18): p. 3076-83.

101. Miller, V.A., et al., *Afatinib versus placebo for patients with advanced, metastatic non-small-cell lung cancer after failure of erlotinib, gefitinib, or both, and one or two lines of chemotherapy (LUX-Lung 1): a phase 2b/3 randomised trial.* Lancet Oncol, 2012. **13**(5): p. 528-38.

102. Godin-Heymann, N., et al., *The T790M "gatekeeper" mutation in EGFR mediates resistance to low concentrations of an irreversible EGFR inhibitor.* Mol Cancer Ther, 2008. **7**(4): p. 874-9.

103. Ward, R.A., et al., *Structure- and reactivity-based development of covalent inhibitors of the activating and gatekeeper mutant forms of the epidermal growth factor receptor (EGFR).* J Med Chem, 2013. **56**(17): p. 7025-48.

104. Cross, D.A., et al., *AZD9291, an irreversible EGFR TKI, overcomes T790M-mediated resistance to EGFR inhibitors in lung cancer.* Cancer Discov, 2014. **4**(9): p. 1046-61.

105. Ramalingam, S., et al., *LBA1_PR: Osimertinib as first-line treatment for EGFR mutation-positive advanced NSCLC: updated efficacy and safety results from two Phase I expansion cohorts.* J Thorac Oncol, 2016. **11**(4 Suppl): p. S152.

106. Riely, G.J., et al., *Prospective assessment of discontinuation and reinitiation of erlotinib or gefitinib in patients with acquired resistance to erlotinib or gefitinib followed by the addition of everolimus.* Clin Cancer Res, 2007. **13**(17): p. 5150-5.

107. Chaft, J.E., et al., *Disease flare after tyrosine kinase inhibitor discontinuation in patients with EGFR-mutant lung cancer and acquired resistance to erlotinib or gefitinib: implications for clinical trial design.* Clin Cancer Res, 2011. **17**(19): p. 6298-303.

108. Chmielecki, J., et al., *Optimization of dosing for EGFR-mutant non-small cell lung cancer with evolutionary cancer modeling.* Sci Transl Med, 2011. **3**(90): p. 90ra59.

109. Regales, L., et al., *Dual targeting of EGFR can overcome a major drug resistance mutation in mouse models of EGFR mutant lung cancer.* J Clin Invest, 2009. **119**(10): p. 3000-10.

110. Janjigian, Y.Y., et al., *Dual inhibition of EGFR with afatinib and cetuximab in kinase inhibitor-resistant EGFR-mutant lung cancer with and without T790M mutations.* Cancer Discov, 2014. **4**(9): p. 1036-45.

111. Yang, S., et al., *Association with HSP90 inhibits Cbl-mediated down-regulation of mutant epidermal growth factor receptors.* Cancer Res, 2006. **66**(14): p. 6990-7.

112. Johnson, M.L., et al., *Phase I/II Study of HSP90 Inhibitor AUY922 and Erlotinib for EGFR-Mutant Lung Cancer With Acquired Resistance to Epidermal Growth Factor Receptor Tyrosine Kinase Inhibitors.* J Clin Oncol, 2015. **33**(15): p. 1666-73.

113. Seto, T., et al., *Erlotinib alone or with bevacizumab as first-line therapy in patients with advanced non-squamous non-small-cell lung cancer harbouring EGFR mutations (JO25567): an open-label, randomised, multicentre, phase 2 study.* Lancet Oncol, 2014. **15**(11): p. 1236-44.

114. Gettinger, S.N., et al., *Overall Survival and Long-Term Safety of Nivolumab (Anti-Programmed Death 1 Antibody, BMS-936558, ONO-4538) in Patients With Previously Treated Advanced Non-Small-Cell Lung Cancer.* J Clin Oncol, 2015. **33**(18): p. 2004-12.

115. Akbay, E.A., et al., *Activation of the PD-1 pathway contributes to immune escape in EGFR-driven lung tumors.* Cancer Discov, 2013. **3**(12): p. 1355-63.

116. Cheung, H.W., et al., *Systematic investigation of genetic vulnerabilities across cancer cell lines reveals lineage-specific dependencies in ovarian cancer.* Proceedings of the National Academy of Sciences of the United States of America, 2011. **108**(30): p. 12372-7.

117. Dunn, G.P., et al., *In vivo multiplexed interrogation of amplified genes identifies GAB2 as an ovarian cancer oncogene.* Proc Natl Acad Sci U S A, 2014. **111**(3): p. 1102-7.

118. Mali, P., K.M. Esvelt, and G.M. Church, *Cas9 as a versatile tool for engineering biology.* Nat Methods, 2013. **10**(10): p. 957-63.

119. Hsu, P.D., E.S. Lander, and F. Zhang, *Development and applications of CRISPR-Cas9 for genome engineering.* Cell, 2014. **157**(6): p. 1262-78.

120. Shalem, O., et al., *Genome-scale CRISPR-Cas9 knockout screening in human cells.* Science, 2014. **343**(6166): p. 84-7.

121. Sos, M.L., et al., *PTEN loss contributes to erlotinib resistance in EGFR-mutant lung cancer by activation of Akt and EGFR.* Cancer Res, 2009. **69**(8): p. 3256-61.

122. de Bruin, E.C., et al., *Reduced NF1 expression confers resistance to EGFR inhibition in lung cancer.* Cancer Discov, 2014. **4**(5): p. 606-19.

123. Pirazzoli, V., et al., *Acquired resistance of EGFR-mutant lung adenocarcinomas to afatinib plus cetuximab is associated with activation of mTORC1.* Cell Rep, 2014. **7**(4): p. 999-1008.

124. Fuchs, A., et al., *Tuberous-sclerosis complex-related cell signaling in the pathogenesis of lung cancer.* Diagn Pathol, 2014. **9**: p. 48.

125. Huang, S., et al., *MED12 controls the response to multiple cancer drugs through regulation of TGF-beta receptor signaling.* Cell, 2012. **151**(5): p. 937-50.

126. Busser, B., et al., *Amphiregulin promotes BAX inhibition and resistance to gefitinib in non-small-cell lung cancers.* Mol Ther, 2010. **18**(3): p. 528-35.

127. Sen, B. and F.M. Johnson, *Regulation of Src Family Kinases in Human Cancers.* Journal of Signal Transduction, 2011. **2011**: p. 1-14.

128. Confalonieri, S., et al., *Alterations of ubiquitin ligases in human cancer and their association with the natural history of the tumor.* Oncogene, 2009. **28**(33): p. 2959-68.

129. Hao, Z., et al., *The E3 ubiquitin ligase Mule acts through the ATM-p53 axis to maintain B lymphocyte homeostasis.* J Exp Med, 2012. **209**(1): p. 173-86.

130. Hall, J.R., et al., *Cdc6 stability is regulated by the Huwe1 ubiquitin ligase after DNA damage.* Mol Biol Cell, 2007. **18**(9): p. 3340-50.

131. Zhao, X., et al., *The HECT-domain ubiquitin ligase Huwe1 controls neural differentiation and proliferation by destabilizing the N-Myc oncoprotein.* Nat Cell Biol, 2008. **10**(6): p. 643-53.

132. Inoue, S., et al., *Mule/Huwe1/Arf-BP1 suppresses Ras-driven tumorigenesis by preventing c-Myc/Miz1-mediated down-regulation of p21 and p15.* Genes Dev, 2013. **27**(10): p. 1101-14.

133. Ma, W., et al., *Tumour suppressive function of HUWE1 in thyroid cancer.* J Biosci, 2016. **41**(3): p. 395-405.

134. Chen, D., et al., *ARF-BP1/Mule is a critical mediator of the ARF tumor suppressor.* Cell, 2005. **121**(7): p. 1071-83.

135. Vaughan, L., et al., *HUWE1 Ubiquitylates and Degrades the RAC Activator TIAM1 Promoting Cell-Cell Adhesion Disassembly, Migration, and Invasion.* Cell Rep, 2015. **10**(1): p. 88-102.

136. Bernassola, F., et al., *The HECT family of E3 ubiquitin ligases: multiple players in cancer development.* Cancer Cell, 2008. **14**(1): p. 10-21.

137. Matsunaga-Udagawa, R., et al., *The scaffold protein Shoc2/SUR-8 accelerates the interaction of Ras and Raf.* J Biol Chem, 2010. **285**(10): p. 7818-26.

138. Shimamura, A., et al., *Rsk1 mediates a MEK-MAP kinase cell survival signal.* Curr Biol, 2000. **10**(3): p. 127-35.

139. Kobayashi, S., et al., *Transcriptional profiling identifies cyclin D1 as a critical downstream effector of mutant epidermal growth factor receptor signaling.* Cancer Res, 2006. **66**(23): p. 11389-98.

140. Tsai, S.Q., et al., *Dimeric CRISPR RNA-guided FokI nucleases for highly specific genome editing.* Nat Biotechnol, 2014. **32**(6): p. 569-76.

141. Ivey, J.W., et al., *Improving cancer therapies by targeting the physical and chemical hallmarks of the tumor microenvironment.* Cancer Lett, 2016. **380**(1): p. 330-9.

142. Kerbel, R.S., *Human tumor xenografts as predictive preclinical models for anticancer drug activity in humans: better than commonly perceived-but they can be improved.* Cancer Biol Ther, 2003. **2**(4 Suppl 1): p. S134-9.

143. Sporn, J.R. and S.A. Bilgrami, *Weekly paclitaxel plus Herceptin in metastatic breast cancer patients who relapse after stem-cell transplant.* Ann Oncol, 1999. **10**(10): p. 1259-60.

144. Tang, Y., et al., *Human-derived IgG level as an indicator for EBV-associated lymphoma model in Hu-PBL/SCID chimeras.* Virol J, 2011. **8**: p. 213.

145. Bankert, R.B., et al., *Humanized mouse model of ovarian cancer recapitulates patient solid tumor progression, ascites formation, and metastasis.* PLoS One, 2011. **6**(9): p. e24420.

146. Bernard, D., M. Peakman, and A.C. Hayday, *Establishing humanized mice using stem cells: maximizing the potential.* Clin Exp Immunol, 2008. **152**(3): p. 406-14.

147. Maeder, M.L., et al., *CRISPR RNA-guided activation of endogenous human genes.* Nat Methods, 2013. **10**(10): p. 977-9.

148. Lee, H.J., et al., *Drug resistance via feedback activation of Stat3 in oncogene-addicted cancer cells.* Cancer Cell, 2014. **26**(2): p. 207-21.

149. Kim, S.M., et al., *Activation of IL-6R/JAK1/STAT3 signaling induces de novo resistance to irreversible EGFR inhibitors in non-small cell lung cancer with T790M resistance mutation.* Mol Cancer Ther, 2012. **11**(10): p. 2254-64.

150. Li, R., et al., *Niclosamide overcomes acquired resistance to erlotinib through suppression of STAT3 in non-small cell lung cancer.* Mol Cancer Ther, 2013. **12**(10): p. 2200-12.

151. Li, R., et al., *Inhibition of STAT3 by niclosamide synergizes with erlotinib against head and neck cancer.* PLoS One, 2013. **8**(9): p. e74670.

152. Pierce, N.W., et al., *Detection of sequential polyubiquitylation on a millisecond timescale.* Nature, 2009. **462**(7273): p. 615-9.

153. Harper, J.W. and M.K. Tan, *Understanding cullin-RING E3 biology through proteomics-based substrate identification.* Mol Cell Proteomics, 2012. **11**(12): p. 1541-50.

154. Coyaud, E., et al., *BioID-based Identification of Skp Cullin F-box (SCF)beta-TrCP1/2 E3 Ligase Substrates.* Mol Cell Proteomics, 2015. **14**(7): p. 1781-95.

155. Wu, Z., et al., *Nuclear protein IkappaB-zeta inhibits the activity of STAT3.* Biochem Biophys Res Commun, 2009. **387**(2): p. 348-52.

156. Totzke, G., et al., *A novel member of the IkappaB family, human IkappaB-zeta, inhibits transactivation of p65 and its DNA binding.* J Biol Chem, 2006. **281**(18): p. 12645-54.